Charles University in Prague
Faculty Of Science

Study Program: Immunology

Bc. Sıla Azak

Charakterizace imunitní odpovědi proti viru SARS-CoV-2

Characterization of the immune responses against SARS-CoV-2 virus

Diploma Thesis

Supervisor: MUDr. Zora Mělková, PhD

Prague 2024

Declaration

I hereby declare that my thesis represents my own original research work. Wherever the contribution of others is involved, every effort is made to indicate this clearly including reference to the literature. This thesis contains no material that has been submitted previously, in whole or in part, for the award of any other academic degree or diploma.

Prague, 07.08.2024 Sıla Azak

Firstly, I want to express my gratitude to Dr. Mělková for her invaluable help, guidance, and patience throughout this project. I would also like to thank Monika Kaplanová and Zvikomborero Manjengwah, our laboratory technicians, for their assistance.

Special thanks to Mgr. Martin Chmel from the Military Health Institute, Military Medical Agency, Prague and Department of Infectious Diseases, First Faculty of Medicine, Charles University and Military University Hospital Prague for providing the SARS-CoV-2.

I am grateful to Prof. Jan Černý, Mgr. Lenka Doubravská, Ph.D, Mgr. Anna Maria Frontino, and Mgr. Zuzana Brůhová for their support and help with the histology samples.

Abstrakt

SARS-CoV-2 (Severe Acute Respiratory Syndrome Coronavirus-2) je obalený virus s jednovláknovou RNA z čeledi Coronaviridae. Tento virus byl příčinou celosvětové pandemie vyhlášené v roce 2019. Je spojen se zápalem plic a syndromem akutní respirační tísně (ARDS), což je stav charakterizovaný poškozením plic a respiračním selháním, které je podmíněno nekontrolovaným zánětem v důsledku disregulované imunitní odpovědi. SARS-CoV-2 infikuje člověka prostřednictvím Spike (S) proteinu, který se váže na lidský angiotenzin-konvertující enzym 2 (hACE2) exprimovaný na různých buňkách včetně alveolárních epiteliálních buněk. V plicích vazba SARS-CoV-2 na hACE2 aktivuje imunitní buňky, zvyšuje produkci cytokinů a aktivuje další zánětlivou odpověď. COVID-19 je charakterizován zvýšenými koncentracemi IL-2, IL-6, IL-8, TNF-α a IFN-γ v plazmě pacientů a závažnost onemocnění koreluje s vysokou expresí IL-6 a TNF-α spolu se slabou odpovědí interferonu 1. typu. Heme arginát je látka obsahující hem, která se používá k léčbě akutních porfyrií. Dřívější články popsaly, že hem a indukce HO-1 inhibují růst a replikaci různých RNA a DNA virů. Nedávno Dr. Mělková se spolupracovníky pozorovali inhibici SARS-CoV-2 v tkáňových kulturách a změněný průběh infekce u myší K18-hACE2. Cílem této práce je charakterizovat hladiny cytokinů TNF-α, IFN-γ, IFN-α, IL-6, IL-10, IL-22, IL-1β, IL-17A, IL-2, IL12-p70 a IL-4 produkovaných v odpověď na infekci SARS-CoV-2 u těchto myší.

Klíčová slova: SARS-CoV-2, hem arginát, cytokiny, K18-hACE2 mice

Abstract

Severe Acute Respiratory Syndrome Coronavirus-2 (SARS-CoV-2) is an enveloped, single-stranded RNA virus, a member of the Coronaviridae family. This virus was declared the cause of a global pandemic in 2019. It is associated with pneumonia and Acute Respiratory Distress Syndrome (ARDS), a condition characterized by lung injury and respiratory failure underlined by uncontrolled hyperinflammation resulting from deregulated immunity. SARS-CoV-2 infects human through the Spike (S) protein, which binds to the human angiotensin-converting enzyme 2 (hACE2), expressed on the membrane of different cell types, including the alveolar epithelial cells. In the lungs, the binding of SARS-CoV-2 to hACE2 triggers the immune cells, increases cytokine production, and activates other inflammatory responses. COVID-19 has been characterized by higher concentrations of IL-2, IL-6, IL-8, TNF-α, and IFN-γ in patients' plasma. The disease severity is correlated with high expression of IL-6 and TNF-α together with a poor type 1 interferon response. Heme arginate is a heme compound that is used for the treatment of acute porphyrias. Previous papers have described that heme and HO-1 induction inhibited the growth and replication of various RNA and DNA viruses. Lately, Dr. Mělková and colleagues have observed that heme arginate inhibited SARS-CoV-2 in tissue culture and modified the course of infection in K18-hACE2 mice. This thesis aims to characterize levels of TNF-α, IFN-γ, IFN-α, IL-6, IL-10, IL-22, IL-1β, IL-17A, IL-2, IL12-p70 and IL-4 cytokines produced in response to SARS-CoV-2 in these mice.

Keywords: SARS-CoV-2, Heme Arginate, Cytokines, K18-hACE2 mice

Contents

List of Abbreviations

Abbreviation	Meaning in English
ALI	Acute Lung Injury
AP-1	Activator Protein 1
APCs	Antigen Presenting Cells
ARDS	Acute Respiratory Distress Syndrome
CS	Cytokine Storm
DMEM	Dulbecco's Modified Eagle Medium
eNOS	Endothelial Nitric Oxide Synthase
ERK	Extracellular Signal-Regulated Kinase
FBS	Fetal Bovine Serum
GM-CSF	Granulocyte-Macrophage Colony Stimulator Factor
GMO	Genetically Modified Organism
HA	Heme Arginate
h-ACE2	Human Angiotensin-Converting Enzyme 2
HO	Heme Oxygenase
IFN	Interferon
IFNAR	Interferon-α/β Receptor
IKK	Inhibitor of κB (IκB) Kinase
IL	Interleukin
iNOS	Induced Nitric Oxide Synthase
IRF	Interferon Regulatory Factor
ISG	Interferon Stimulated Gene
ISGF	IFN-Stimulated Gene Factor
ISREs	IFN-Stimulated Response Elements
JAK	Janus Kinase
JNK	Jun N-Terminal Kinase
MAPK	Mitogen-Activated Protein Kinase

MAVS	Mitochondrial Antiviral-Signaling Protein
MDA5	Melanoma Differentiation Associated Protein-5
MEK	Mitogen-Activated Protein Kinase Kinase
NETs	Neutrophil Extracellular Traps
NF-κB	Nuclear Factor Kappa B
NK	Natural Killer
NO	Nitric Oxide
NOS	Nitric Oxide Synthase
NSP	Non-Structural Proteins
ORF	Open Reading Frame
p.i	Post Infection
PAMPs	Pathogen-Associated Molecular Patterns
PBS	Phosphate-Buffered Saline
PRRs	Pattern Recognition Receptors
R	Remdesivir
RLR	RIG-1 Like Receptor
ROS	Reactive Oxygen Species
SARS-CoV-2	Severe Acute Respiratory Syndrome Coronavirus-2
STAT	Signal Transducers and Activators
STING	Stimulator of Interferon Genes
TBK	TANK-Binding Kinase
Th	T helper
TLR	Toll-Like Receptor
TMPRSS2	Transmembrane Serine Protease 2
TNF	Tumor Necrosis Alpha
TNFR	Tumor Necrosis Factor Receptor
TRAF	Tumor Necrosis Factor Receptor- Associated Factor
Tregs	Regulatory T Cells
TYK	Tyrosine Kinase

1 Introduction

In late 2019, Severe Acute Respiratory Syndrome Coronavirus-2 (SARS-CoV-2) caused a pandemic that affected the people worldwide. The virus generally enters the human body through the upper respiratory tract and activates immune system, leading to increased cytokine production and other defense strategies.

The SARS-CoV-2 binds to the host cell membrane using the spike protein, allowing the virus to attach to the human angiotensin-converting enzyme 2 (hACE2) receptor and fuse with the membrane of the host cell. Once bound, it is recognized by the pattern recognition receptors (PRRs), activating macrophages, NK cells, and other immune cells to release chemokines and cytokines. It can also infect cells through phagocytosis of apoptotic cells infected with the virus. These processes induce rapid innate immune responses.

Excessive production of proinflammatory cytokines leads to a hyperinflammatory state, referred to as a cytokine storm (CS), which may result in the multiorgan damage and mortality in patients infected with SARS-CoV-2. Patients who experience CS may also suffer from CS-induced cytokine release syndrome and acute respiratory distress syndrome (Rabaan et al., 2021).

The laboratory of Dr. Zora Mělková has discovered that a clinically used compound Normosang, containing heme arginate, can inhibit the replication of SARS-CoV-2 in Vero cells. In patients with COVID-19, Normosang improved saturation of blood with oxygen and/or reduced the need for oxygen supply, and prevented the worsening of the clinical state, progression to Intensive care unit (ICU), and artificial pulmonary ventilation (unpublished results). In mice infected with SARS-CoV-2, administration of Normosang revealed varying effects on virus replication and spread.

2 Objectives of Work

This project aims to characterize the effects of Heme Arginate on levels of selected cytokines produced in response to SARS-CoV-2 infection, namely IL-1β, IL-6, TNF-α, IFN-α, IFN-γ, IL-2, IL-17A, IL-12p70, IL-10, IL-4, IL-22.

3 Literature Review

3.1 SARS-CoV-2

SARS-CoV-2 is a member of the Coronaviridae family and belongs to the subgenus Sarbecovirus. It is an enveloped virus with a single-stranded positive-sense RNA genome. The SARS-CoV-2 genome contains 14 open reading frames (ORF) encoding 29 proteins; the first two ORFs encoding nonstructural proteins represent almost 70% of the virus genome, while the remaining 30% of the ORFs encodes various accessory proteins and namely four structural proteins including membrane (M), envelope (E), spike (S), nucleocapsid (N) proteins.

3.1.1 SARS-CoV-2 Replication Cycle

3.1.1.1 Cell Entry

The SARS-CoV-2 virus enters the host cell by binding to the hACE2 as receptor using the S protein, which consists of two parts: S1 and S2. The hACE2 is the primary receptor for SARS-CoV-2. This attachment triggers the priming of the S1 at the S1/S2 junction by furin or endosomal protease. This process exposes S2, which is then cleaved by the transmembrane serine protease 2 (TMPRSS2) and reveals the fusion peptide of the S2 subunit. The cleavage permanently changes the conformation of the S protein and allows the S2 subunit to integrate into the host membrane. Afterward, it guides the fusion of the viral and cellular membranes. It has been reported that CD147, a transmembrane glycoprotein, can also mediate the cellular entry of SARS-CoV-2 into cells. The interaction between the virus and its receptors determines the tissue tropism, disease development, and cross-species transmission and regulates the infection (Bakhiet & Taurin, 2021).

3.1.1.2 Expression of Viral Genes

Coronavirus has one of the largest RNA genomes among all RNA virus families and encodes about 29 proteins. The genome of a virus contains various types of proteins. These include non-structural proteins responsible for the enzymatic activities required for viral replication, and structural proteins (S, E, N, and M proteins) that provide the virus its physical structure. There are

also accessory proteins that don't participate in viral replication but instead interfere with the host's innate immune responses (Ju et al., 2021). Coronavirus is a virus that can harm or kill the host cell as part of its replication process. Cell death occurs when the virus takes control over the host cell machinery and genetic material, which allows the virus to replicate itself more efficiently (Marston et al., n.d.).

Cells that express the ACE2 and TMPRSS2 are highly susceptible to SARS-CoV-2 infection. Once the virus enters these cells, the viral genome is unpacked from bound viral N proteins by cellular proteases within the cytoplasm. The viral genome functions like mRNA, first allowing translation of two polypeptides from the open frame 1a (ORF1a) and ORF1b. To initiate replication and transcription of the viral genome, these polypeptides are cleaved by two viral proteases into sixteen non-structural proteins. The viral genome encodes four structural proteins and six accessory proteins. Their translation requires newly synthesized subgenomic RNAs. SARS-CoV-2 is a virus that replicates exclusively in the cytoplasm of infected cells. After continuous transcription of gRNA, newly produced gRNA is encapsulated with N proteins, enclosed by a viral envelope, and released from the infected cells (Brant et al., 2021).

3.1.1.3 Morphogenesis of New Virions

Research on morphogenesis has revealed that after the virus entry into the cell, mediated by the S protein, the replication cycle starts with a synthesis of viral proteins that organize and catalyze viral RNA synthesis. After synthesis of the individual building blocks (proteins, gRNA), viral morphogenesis starts when the virus-induced double-membrane structures are formed from the rough endoplasmic reticulum which is known as double-membrane vesicles (Barreto-Vieira et al., 2022). The N protein helps in the formation of helical structures of positive-sense gRNA in the cytoplasm. It also interacts with the M protein, which is hydrophobic and present in the endoplasmic reticulum-Golgi intermediate compartment. This interaction helps in the direct assembly and budding of mature virions. Finally, these virions are transported to the cell surface in vesicles and then secreted through exocytosis from the plasma membrane (Zhou et al., 2023).

.

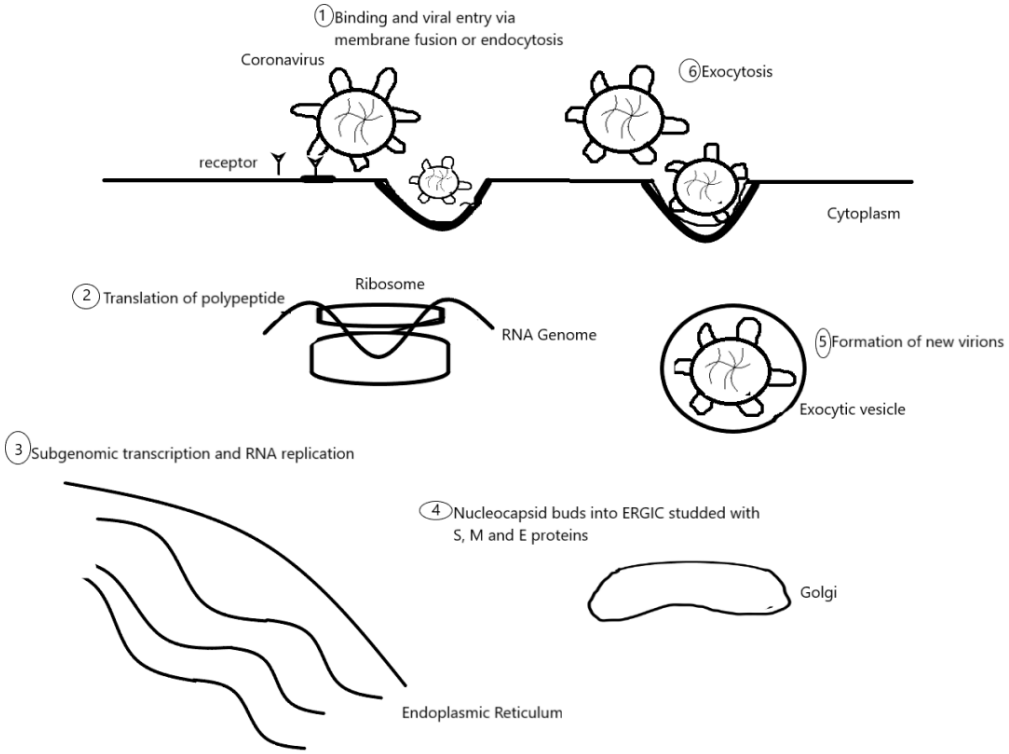

Figure 1 Morphogenesis of New Virions

3.2 Immune Response Against SARS-CoV-2

As mentioned earlier, SARS-CoV-2 is an RNA virus that replicates in the host cytoplasm. Essential steps in triggering immune responses against an RNA virus involve the recognition of the viral RNA in cytoplasm, the expression of interferons and the genes they induce (ISGs), and the subsequent activation of the adaptive immune system.

3.2.1 Toll-Like Receptors

Toll-like receptors (TLRs) are a type of pattern recognition receptor (PRR) located in the cell membrane or in the endosome. They activate the host innate immune responses to viruses and are found on immune system cells and epithelial cells. TLR3 recognizes double-stranded RNA, TLR7 and TLR8 recognize single-stranded RNA, and TLR9 is associated with

unmethylated CpG DNA. When activated, these receptors initiate signaling pathways that lead to the translocation of Interferon Regulatory Factors (IRFs) and nuclear factor-kappa B (NF-κB) into the cell nucleus, where they trigger expression of interferons (IFNs) and inflammatory cytokines, respectively (Kawasaki & Kawai, 2014).

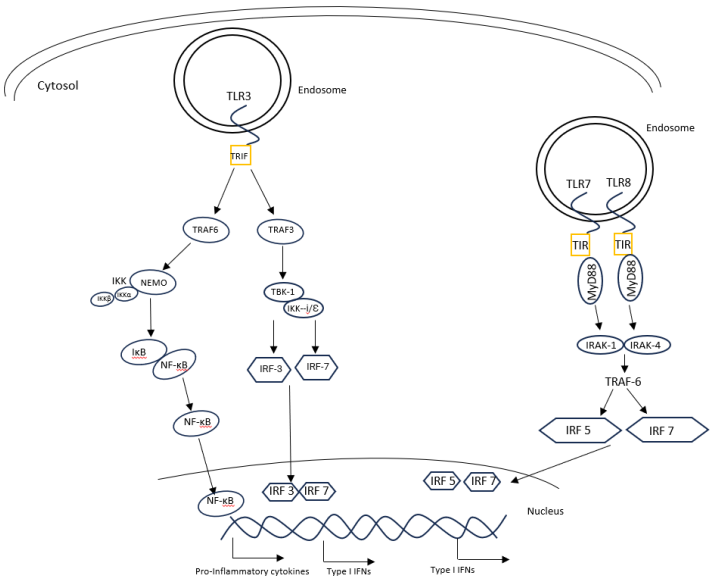

Figure 2 TLR Signaling

3.2.2 RIG-I Like Receptors and Melanoma Differentiation- Associated Protein 5 (RLRs and MDA5)

RLRs and MDA5 belong to the PRR family and are responsible for detecting viral RNA in the cytoplasm. The signaling pathways from these receptors converge in the mitochondrial antiviral-signaling protein pathway (MAVS). RLR-MAVS interacts with STING (stimulator of interferon genes) and TRAF3 (TNFR-associated factor 3), which then activate TBK1 (TANK-binding kinase 1) and IKK (inhibitor of κB (IκB) kinase) kinases. TBK1 phosphorylates the transcription factor IRF3, and IKK phosphorylates the NF-κB, allowing them to dimerize and translocate into the nucleus (Gusev et al., 2022).

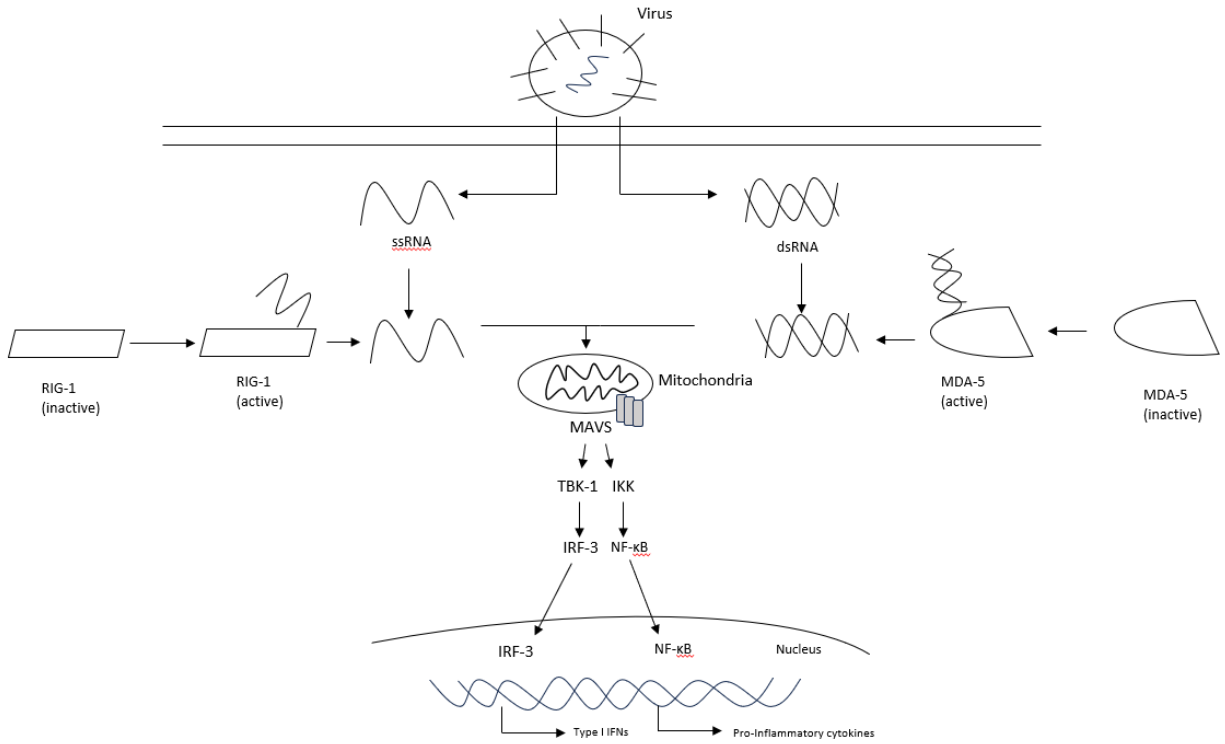

Figure 3 RLR and MDA-5 Signaling Pathway

3.2.3 Interferons

Interferons (IFNs) are proteins produced by animal cells that are usually associated with the first line of defense against viruses. IFNs are classified into three types based on sequence homology and functional properties: type I, II, and III. Type I IFNs include IFN-α, IFN-β, and IFNε, IFNω, and IFNτ, Type II IFNs include IFN-γ and Type III IFNs include IFN-λ (Park & Iwasaki, 2020). IFNα and IFNβ are expressed by innate immune cells, particularly plasmacytoid dendritic cells, and non-immune cells, like fibroblast and epithelial cells, respectively. Importantly, all the infected non-immune cells can produce IFNβ (Ivashkiv & Donlin, 2014). IFN-γ is a type II interferon produced by T lymphocytes, macrophages, mucosal epithelial cells, or natural killer cells (Ding et al., 2022).

Type I and III IFNs are primary defense proteins against viral infections. Cells infected by viruses and innate immune cells recognize viral infection through PRRs and produce type I

and III IFNs. The main difference between type I and type III IFN signaling is that type I IFN signaling is rapid, transient, and systemic, while type III IFN signaling is less potent, slower, sustained and limited to the epithelial and barrier surfaces. In this way, type III IFNs serve as a primary defense against viruses at epithelial surfaces, causing smaller collateral damage than the more powerful type I IFNs (Choi & Shin, 2021; Lazear et al., 2019).

As mentioned above translocation of IRF3 and NF-κB into the nucleus results in the production of Type I IFNs. The interferon-α/β receptor 1-2 (IFNAR1-2) is expressed by neighboring cells, including uninfected ones, allowing them to respond to IFN. The receptor is associated with Janus Kinase 1 (JAK1) and tyrosine kinase 2 (TYK2). When the receptor dimerizes, it leads to the autophosphorylation of JAK1, which phosphorylates signal transducers and activators 1 (STAT1) and STAT2 proteins. The phosphorylated STAT1/2 recruits IRF9 to form the transcription factor complex called IFN-stimulated gene factor 3 (ISGF3). ISGF3 then moves to the nucleus where it binds to IFN-stimulated response elements (ISREs) in gene promoters of ISGs, leading to their transcription (Platanias, 2005; Yang & Li, 2020).

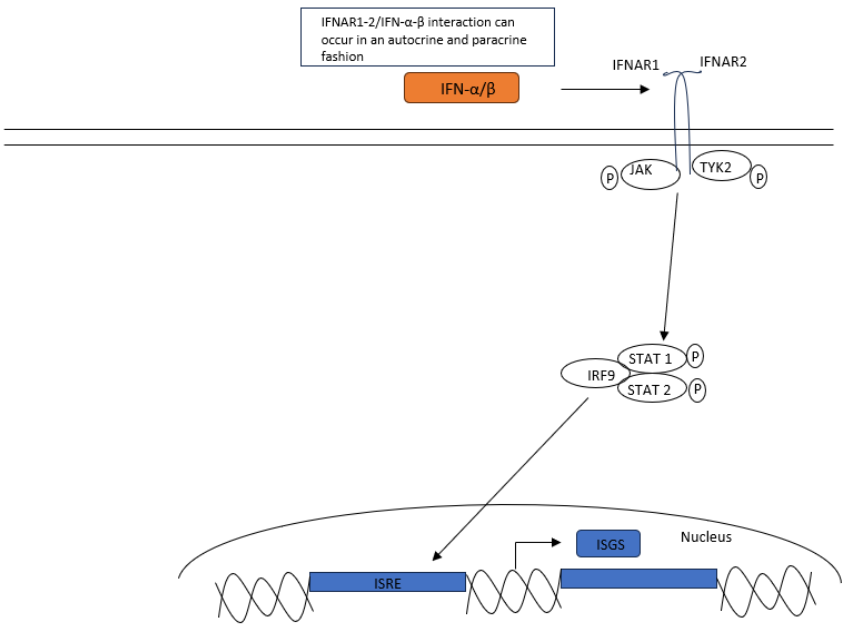

Figure 4 IFN signaling

3.2.4 IL-1β

Interleukin-1β is a pro-inflammatory cytokine that plays an important role in the host defense against infection and injury. It is secreted by neutrophils, macrophages and infiltrating cytokines. It is a member of the IL-1 Receptor family. In response to a triggering stimulus it is produced in inactive form, pro-IL-1β, later active caspase-1 cleaves pro-IL-1β into its mature and active form, IL-1β (Boraschi et al., 2018; Montazersaheb et al., 2022). Once it is secreted, it triggers the inflammation-related signaling pathways which lead to the activation of various transcription factors, namely, NF-κB, activator protein-1 (AP-1), c-JUN N-terminal kinase (JNK), p38, mitogen-associated protein kinases (MAPK), extracellular signal-regulated kinases, and interferon-regulating genes (Montazersaheb et al., 2022).

The process of IL-1β secretion is not completely understood. Various mechanisms and pathways have been proposed, including passive release by dying cells, translocation across the membrane, translocation in intracellular vesicles followed by exocytosis, and release via exosomes or microvesicles. It has been suggested that monocytes can choose between these mechanisms and pathways based on the strength of the signals they receive (Sitia & Rubartelli, 2018).

3.2.5 TNF Alpha

Tumor necrosis factor-alpha (TNF-α) is a type of pro-inflammatory cytokine that is produced mainly by macrophages and monocytes during acute inflammation, but other cell types like T and B lymphocytes, mast cells, NK cells, neutrophils are also secreting TNF-α. It is known to be upregulated in cases of acute lung injury. This upregulation can trigger cytokine release syndrome and facilitate the interaction of SARS-CoV-2 with hACE2 (Guo et al., 2022).

TNF-α exerts its effects by binding to two distinct receptors, TNFR1 (p55) and TNFR2 (p75), present on the surface of cells. TNFR1 is expressed in all human tissues, while TNFR2 is predominantly found in immune cells, neurons, and endothelial cells. The interaction with TNFR1 is important for promoting inflammatory responses and the expansion of effector T cells, while interaction with TNFR2 is associated with anti-inflammatory actions and promoting cell survival. Signaling via TNFR1 also triggers the activation of transcription factors such as NF-κB and AP-1. Alternatively, it can lead to cell death through activation of caspase 8, resulting in apoptosis. By inhibiting TNF-α signaling, various anti-TNF-α biological treatments prime naïve CD4+ T cells

towards a regulatory phenotype characterized by high expression of IL-10 and reduced IFN-γ production (Holbrook et al., 2019; Liang et al., 2022; Manohar, 2024).

3.2.6 IL-10 and IL-22

IL-10 family of cytokines comprises nine members, including IL-19, IL-20, IL-22, IL-24, and IL-26, as well as the more distantly related IL-28A, IL-28B, and IL-29 (Xu et al., 2021). These cytokines are produced by both innate and adaptive immune cells, and they serve as regulatory and effector molecules in the immune system. IL-10 is secreted by leukocytes such as dendritic cells, T and B cells, macrophages, and Natural Killer cells. Meanwhile, IL-22 is primarily produced by myeloid cells, particularly by T cell subsets and group 3 innate lymphoid cells (ILC3s) (Ouyang & O'Garra, 2019).

IL-10 primarily suppresses myeloid cells by inhibiting the production of proinflammatory cytokines and antigen-presenting cells (APCs). Additionally, IL-10 directly inhibits memory Th17 and Th2 cells while promoting the survival and function of Foxp3+ regulatory T cells (Tregs).IL-22 exhibits both protective and pro-inflammatory effects. It can enhance tissue regeneration and wound healing, thereby offering potential therapeutic benefits in diseases associated with tissue damage (Ouyang & O'Garra, 2019).

The IL-22R axis protects against bacterial and viral infections in the lungs. During viral infections, IL-22R signaling induces secretion of several chemokine that aid in the recruitment of neutrophils to the site of infection. Neutrophils might be beneficial for the clearance of the infected cells and by NETs trapping the viruses or they can lead to hyperinflammatory conditions. Epithelial cells of the lung and some hematopoietic cells produce IL-22BP, which binds to IL-22 with greater affinity than the membrane receptor and regulates the potentially harmful interaction between IL-22 and IL-22R (Albayrak et al., 2022).

3.2.7 IL-17A

IL-17A is a pro-inflammatory cytokine released by various types of cells, including Th17 cells, CD8+ T cells, NK T cells, innate lymphoid cells, neutrophils, and γΔ-T cells. These cells play a crucial role in the adaptive immune responses during viral infections. Once Th17 cells are

activated, they trigger the release of inflammatory cytokines and assist in recruiting monocytes and neutrophils to the site of infection.

IL-17A, also referred to as IL-17, family consisting of 6 members. It is particularly important because it can increase inflammatory responses by activating downstream cytokines such as IL-6, IL-8, IL-1, TNF-α, and MCP-1. IL-17 acts through the IL-17 receptor by activating NF-κB and MAPK pathways, leading to the production of proinflammatory cytokines and chemokines. In viral infections, there is a link between IL-6 and IL-17A such that excessive IL-6 production can enhance the generation of IL-17A-producing Th17 cells. The differentiation of Th17 cells is mediated by JAK-STAT pathways, and signals from IL-6 and IL-23 can induce Th17 cell polarization of the naïve CD4+ T cells (Das & Khader, 2017; Montazersaheb et al., 2022).

Several studies have demonstrated that IL-17 promotes the accumulation of neutrophils in the lungs during infections. Conversely, hACE2 inhibits STAT3, which diminishes the infiltration of neutrophils. This indicates that hACE2 plays a role in regulating the host inflammatory response to infections by counteracting the effects of IL-17A (Orlov et al., 2020).

3.2.8 IL-2 and IL-4

IL-2 is responsible for regulation of white blood cells and lymphocytes. It binds to the IL-2 receptor with modest affinity on lymphocytes. Activated CD4+ T cells and CD8+ T cells are the primary producers of IL-2. When APCs activate Th cells and cytotoxic cells due to SARS-CoV-2 infection in the lungs, the IL-2 family is attached to IL-2R, causing activation of the JAK-STAT pathway. This leads to an inflammatory response, including fibrin formation and lung fibrosis, activation of a cytokine cascade, and fluid leak from the vessels into the alveoli, which in turn causes acute respiratory distress.

IL-4 belongs to the same cytokine family as IL-2 and both cytokines participate in the gamma chain CD132. The primary producers of IL-4 are Th2 cells, mast cells, basophils, and eosinophils. It triggers the development of Th2 cells from Th0 cells, and these Th2 cells demonstrate a positive feedback loop where they produce more IL-4 after being activated by the cytokine. IL-4 is an important cytokine in inflammatory response and can increase lung damage

by activating Th1, Th2, and Th17 responses. Recent studies have shown that the levels of IL-4 significantly increase in the lung autopsies of people infected with SARS-CoV-2 (Ghanbari Naeini et al., 2023). IL-4 is a cytokine that can activate the JAK-STAT signaling pathway. When IL-4 is secreted by Th2 cells, it can induce apoptosis by stimulating the STAT signaling pathway. Additionally, IL-4 can suppress the production of other cytokines, including TNF-α and IL-1. (Hasanvand, 2022).

3.2.9 IL-6

IL-6 is the master regulator of inflammation. In inflammatory or infectious conditions, it is secreted by various cell types, primarily macrophages during acute inflammation and T cells during chronic inflammation. Antigen-presenting cells like dendritic cells also produce IL-6, and NF-κB controls its gene expression.

IL-6 has been found to prevent the death of naive T cells and regulate the balance between Treg and Th17, development of self-reactive CD4+ T cell response, and stimulation of cytotoxic T cell activity as well. It is also established that it has a crucial role in B cell differentiation and antibody production. IL-6 is a glycoprotein that can act as both pro-inflammatory and anti-inflammatory (McElvaney et al., 2021; O'Brien et al., 2015).

IL-6 can cause an imbalance in the immune response during COVID-19 by impairing the function of natural killer and cytotoxic CD8+ T cells, which weakens the host antiviral responses. Moreover, it can hinder the differentiation of Tregs and encourage the polarization of Th17-like γ/δ and α/β CD4+ T cells. This leads to uncontrolled inflammation (Zizzo et al., 2022).

3.2.10 IL-12p70

The IL-12 family includes IL-12, IL-23, IL-27, and IL-35, which play a critical role in the development of Th1 cells, they are mainly produced by DCs, macrophages, monocytes, neutrophils, and microglia cells upon stimulation by PAMPs.

IL-12p70 is an immunoregulatory cytokine composed of two covalently-linked subunits, IL-12p35 and IL-12p40. Each subunit is expressed on a different chromosome. IL-12p40 is

expressed by activated monocytes, macrophages, neutrophils, and dendritic cells. It is suggested that in mice, IL-12p40 homodimers act as antagonists to IL-12p70 activity.

IL-12p70 can promote naïve CD4+ T cells to differentiate into Th1 cells while it protects CD4+ Th1 cells from antigen-induced apoptotic death. It can also enhance the generation and activity of cytotoxic T lymphocytes and increase macrophages' antimicrobial activity (Hamza et al., 2010).

3.2.11 Vaccination

SARS-CoV-2 is a highly infectious and constantly evolving virus, so developing an effective and safe vaccine is critical. Vaccines for SARS-CoV-2 are generated to trigger host immune responses consisting of antibodies towards S protein and activated T-lymphocytes. The latest WHO report from 8 August 2023 shows sixteen fully approved vaccine types under two categories; classic and next-generation platform vaccines.

Classic platform vaccines include an inactivated vaccine, live attenuated vaccine, and viral proteins subunits-based vaccines. Next-generation platform vaccines include viral vector-based vaccines, mRNA engineered vaccine, and DNA-based vaccines.

Sinovac, Sinopharm, and Covaxin are types of whole virion-inactivated vaccines. They use β-propiolactone to inactivate the SARS-CoV-2 virus by binding to its genes. Adjuvants are also added to these vaccines to promote a longer immune response. Covovax and Nuvaxovid recombinant vaccines are based on viral protein subunits. They contain recombinant S protein nanoparticles, which trigger both humoral and cellular immune responses. The Janssen COVID-19 Vaccine is a next-generation platform vaccine containing a human recombinant, replication-incompetent adenoviral vector serotype 26 with the S gene sequence of SARS-CoV-2. On the other hand, mRNA vaccines, such as those developed by Pfizer-BioNTech and Moderna, are known for their high efficiency, safety, low cost, and fast production. These vaccines function by allowing cells to produce the S protein, which in turn triggers the production of antibodies (Abulsoud et al., 2023). Additionally, there is ongoing research on live-attenuated vaccine types. Kin-Hang Kok and colleagues are working on a live but defective SARS-CoV-2 virus, which lacks an envelope

and has the ORF8 segment replaced with interferon-beta. This vaccine has been named the Interferon Beta Integrated SARS-CoV-2 (IBIS) vaccine (Abulsoud et al., 2023; Yuen et al., 2023).

3.3 Defense Mechanism of SARS-CoV-2 Against the Immune System

SARS-CoV-2 reveals several mechanisms to evade the host immune responses, including interference with the RIG-1-MAVS pathways which affect interferon response, mitochondrial sabotage, and disturbance of antigen-presentation.

3.3.1 Evasion of Interferons

The SARS-CoV-2 virus contains several ORFs and Non-Structural Proteins (NSPs) that are used to interfere with the host immune responses, particularly the Interferon system. For instance, these NSP1, NSP6, NSP8, NSP12, NSP13, NSP14, NSP15 and ORF3a, ORF6, ORF7a, ORF7b, ORF9b can inhibit the phosphorylation of TBK1, STAT1, STAT2, and IRF3, as well as the nuclear translocation of IRF3, and STAT1 resulting in the blockage of the Interferon pathway (Rashid et al., 2022).

3.3.2 Impairing Antigen Presentation

SARS-CoV-2 ORF8 encodes a polypeptide that interacts with MHC-1 molecules, leading to their reduced expression. Another study suggested that the ORF6 protein hinders the stimulation of MHC-1 gene expression (Rubio-Casillas et al., 2022).

3.3.3 Mitochondrial Sabotage

SARS-CoV-2 attaches to the mitochondrial import receptor subunit 70 protein, affecting the Type I response and the MAVS-regulated mechanism since MAVS is also present on mitochondria. It has been suggested that SARS-CoV-2 directly interacts with the MAVS protein as well (Rubio-Casillas et al., 2022).

3.4 Heme Arginate

Heme arginate, brand name Normosang, is a compound containing human hemin, and arginine. It is a drug approved for clinical use in treating acute porphyrias.

Heme induces the expression of heme oxygenase 1, which breaks down heme into iron, carbon monoxide, and biliverdin. Biliverdin is then converted into bilirubin by biliverdin reductase. Bilirubin has antioxidant effects that can prevent cytokine storm and help restore endothelial function. Heme-oxygenase (HO) enzymes are responsible for breaking down the heme group; there are three types: inducible HO-1, constitutive HO-2, and a putative mitochondrial HO-3. Among these, HO-1 is the most important isoenzyme in lung diseases. Its expression is triggered by pro-inflammatory cytokines like TNF-α and IL-6, heme, and nitric oxide. HO-1 protects the lungs from inflammation and oxidative stress. It is beneficial in the treatment of Acute Lung Injury (ALI) and ARDS by increasing the levels of anti-inflammatory cytokines such as IL-10 and by reducing the numbers of immune cells that cause inflammation and secretion of inflammatory cytokines like TNF-α and IL-8 (Toro et al., 2022).

On the other hand, arginate is a substrate for NOS isoenzymes. Thus, it can restore the function of NOS (iNOS and eNOS) and the production of NO which could lead to the amelioration of endothelial dysfunction (Guimarães et al., 2021).

One of the features of SARS-CoV-2 infection and replication is oxidative stress and inflammation which contributes to a hyperinflammation state. Oxidative stress reflects an imbalance between production and accumulation of reactive oxygen species (ROS). The presence of HO-1 enables the synthesis of COX, Cytochrome P450, and iNOS enzymes which contributes to inflammation and ROS generation. As a result, HO-1 presence leads to, a reduction of endothelium-derived contracting factors.

HO-1 is an enzyme that is only detected in certain tissues, especially in macrophages where it is responsible for heme degradation (Martínez-Casales et al., 2021).

HO-1 has been found to reveal antiviral effects against different viruses. These effects are mediated by its classical activity, generating heme degradation products (BR, BV, CO, and Fe2+), as well as by the activation of the IFN pathway (Toro et al., 2022).

4. Materials and Methods

4.1 Materials

4.1.1 Chemicals and Solutions

This chapter lists the chemicals and solutions used in the experiments.

4.1.1.1 Chemicals

The following chemicals were used:

Chloroform (Penta)

Ethanol (Penta)

Isopropanol (Penta)

Primers for RT-qPCR (IDT)

4.1.1.2 Solutions

All solutions for work with nucleic acids were prepared in RNase-free water (Sigma), and solutions for work with tissue cultures and for administration to mice were prepared in apyrogenic water for injections (Aqua pro injection). Other solutions were prepared using MilliQ water (25 °C, 18.2 Ω). Solutions for mice and tissue cultures were sterilized by autoclaving or by filtering through a 0.22 μm filter.

- 10x concentrated PBS (phosphate buffered saline) – 1.38M NaCl; 2.7 mM KCl; 1.1mM KH2PO4, 8.1mM Na2HPO4

- RNA Blue (Top-Bio)

4.1.2 Culture and Media and Additives for Tissue Cultures

- 0.1% Trypan Blue

- Trypsin (0.25% solution + 0,05% EDTA v 1x PBS).

- FBS – fetal bovine serum (FBS; Gibco) inactivated for 30 min at 56 °C

- DMEM - Dulbecco's Modified Eagle Medium (DMEM) with a high content of glucose (4.5 g/l), glutamine and pyruvate (Sigma) with the addition of 1·105 U/l Penicillin (Sigma) and 100 mg/l Streptomycin (Sigma)

- 10% FBS-DMEM

4.1.3 Kits

The following commercial kits were used for analysis of levels of selected cytokines and their subsequent analysis;

- Legendplex Multi-Analyte Flow Assay Kit Mouse Anti-Virus Response Panel (Biolegend) - IL-12, IL-1β, IFN-α, IL-6, IL-10

- Legendplex Multi-Analyte Flow Assay Kit Mouse Th Cytokine Panel (12-plex) with Filter Plate V03 (Biolegend) – IFN-γ, TNF-α, IL-2, IL-4, IL-17A, IL-22

4.1.4 Viruses

The following viruses were used for the experiments.

SARS-CoV-2, isolate S-007 from the Biological Defence Department at Těchonín, kindly provided by Mgr. Martin Chmel, Military Health Institute, Military Medical Agency, Prague and Department of Infectious Diseases, First Faculty of Medicine, Charles University and Military University Hospital Prague, for providing the SARS-CoV-2.

4.1.5 Cell Lines

In vitro experiments were performed using green monkey kidney epithelial cells Vero cultured in 10% FBS-DMEM. The cells were maintained in a tissue culture incubator HERA cell CO2 (Heraeus) at 37 °C in an atmosphere with 5% CO2 and 95% humidity.

4.1.6 Mouse Strains

In vivo experiments were performed using mice hemizygous for K18-hACE2(Tg(K18-ACE2)2Prlmn) expressing hACE2 under control of the human keratin 18 (KRT18) promoter. This mouse model was purchased from Jackson Laboratories, USA. The mice for experiments were bred and reared in specific pathogen-free (SPF) conditions in The Center for Experimental Biomodels at the 1st Medical Faculty, Charles University.

4.1.7 Computer Programs

The following programs were used for data acquisition, analysis, and further processing:

- GraphPad Prism 5

- The LEGENDplex™ Data Analysis Software Suite

4.2 Methods

The Virology laboratory at the Institute of Immunology and Microbiology of the 1st Faculty of Medicine, Charles University, led by Dr. Mělková, is authorized to handle genetically modified organisms of risk category 1 and 2 (GMO1, 2) and infectious agents of Biological Safety Level 2 (BSL2). Dr. Mělková also holds a certificate for work with small laboratory animals.

4.2.1 In Vitro Methods

4.2.1.1 Cell Passaging

During passaging, the old medium was first removed from the tissue culture flask of 25 cm^2. The cells were washed with trypsin solution, which was then also removed. Subsequently, 1 ml of fresh trypsin was added, and the cells were incubated for approximately 3 minutes in a tissue culture incubator. After this time, the cells were visually checked if they had detached from the bottom plastic surface of the flask. The trypsin was then inactivated by adding 4 ml of 10% FBS/DMEM. The cell clumps were dispersed by pipetting. Eight ml of new culture medium was then added to the aliquot of the cells and the cells were further cultured.

4.2.1.2 Cell Counting

A 50 µl sample of trypsinized cell suspension (from a total volume of 8 ml) was taken. To this volume, 50 µl of 0.1% trypan blue in 1x concentrated PBS was added; and the viable cells were counted using a light microscope.

4.2.1.3 Infection of Cell Lines

The cells were plated at the density of $0.075x10^6$cells/well in a 24-well plate 24 hours before the infection. For experiments, 0.15×10^6 cells in a 24-well plate were washed with DMEM and infected with 2 different dilutions of virus inocula (200 µl/sample of the 10^{-5} and 10^{-4} dilutions of the original stock, which corresponds to $2x10^8$ and $2x10^9$ E-gene copies/sample, respectively, or 50 and 500 PFU/sample, respectively in DMEM). After 1 h of virus adsorption, the medium was brought to final 2% FBS-DMEM and supplemented with different concentrations of HA (1.25 and 2.5 µl/ml). The cells were then incubated for 24 h at 37°C and 5% CO_2.

The culture medium was aspirated from the wells. For the uninfected cells, 0.5 ml of RNA-blue was added and then transferred to the Eppendorf tube. Then, the wells were rinsed with 1 ml of PBS. This washing step was repeated twice, and finally, 1 ml of media was added.

For the infected wells, they were aspirated, and subsequently, 0,5 ml of media (without FBS) was added and for the uninfected samples another 200 ul of media was added. They were put in an incubator till the virus was added.

5 ul of virus was added to 500 ul of media. After mixing, 20 ul was taken out and added to 2 ml of media (10^4) without FBS. After mixing, 200 ul was taken out and added to 1.8 ml of media (10^5) without FBS. Then, the media was aspirated and 200 ul of the infected media was added to the wells. Finally, it was placed in the incubator and shaken every 10 minutes till Heme Arginate was added.

18 ml of media and 6 ml of FBS serum %10 were mixed and poured into 3 different tubes; 12 ml, 4 ml, and 8 ml for different concentrations of Heme Arginate. From the first tube with 12 ml of FBS and media mix 37.5 ul was removed and 37.5 ul of Heme Arginate was added. 4 ml was taken out from the Heme Arginate and media mixture and added to the second tube with 4 ml of media and FBS mixture. The third tube is used for the non-treated group.

800 ul of Heme Arginate, media, and FBS mixture was added to each of the concentrations and incubated for 24 h.

24h later, media was aspirated, the cells were lysed in 0.5 ml of RNAblue, and the lysate was transferred into Eppendorf tubes and stored in the -80°C.

4.2.2 In Vivo Methods

The work with mice was performed by Dr. Mělková and collaborators. The work was carried out in accordance with European regulations for the transport, housing, and care of laboratory animals (Directive 2010/63/EU on the protection of animals used for scientific purposes). The experiments were approved by the Experimental Animal Use Committee of the 1st Faculty of Medicine, Charles University, and the Ministry of Education of the Czech Republic (experimental protocols No. MSMT-43923/2020-3; MSMT-26151/2022-5). The mice were housed in a housing facility of the 1st Faculty of Medicine accredited by the Ministry of Agriculture of the Czech Republic and monitored daily. All experiments with infectious agents were conducted in a laboratory approved for work at Biological Safety Level 2 with negative pressure and in class IIA laminar flow hoods (Biohazard).

4.2.2.1 Infection of Mice

After an adaptation period of at least 2 weeks, the mice were infected intranasally with 2 x 5 µl of SARS-CoV-2 (10 ul/mouse of the 10^{-4} dilution of the original stock, which corresponds to 10^{8} E-gene copies/mouse or 25 PFU/mouse based on titration in Vero cells). HA was administered intravenously (in the retrobulbar venous plexus) at 2 days p.i. at the dose of 3 µg/g of weight. Remdesivir was administered intraperitoneally at 2 and 3 days p.i. at the dose of 5 and 2.5 µg/g of weight, respectively. Mock-treated mice were administered with sterile PBS.

Mice were divided into 5 groups – control, not infected group; group 0 was infected and mock-treated with PBS; HA, R and HA+R groups were treated with individual compounds. All the manipulations with mice were performed in anesthesia with avertin or narcothan.

4.2.2.2 Euthanasia

The mice were sacrificed 4 days p.i.. In anesthesia, the blood was taken for plasma or serum and the mice were euthanized. Lungs, brain, spleen and kidney were taken and frozen for further purposes. Part of lungs was fixed with 4% paraformaldehyde in PBS.

4.2.2.3 Samples for Analyses

The plasma, lung, and spleen samples from infected and control mice were kindly provided by Dr. Mělková.

4.2.3 Analytical Methods

4.2.3.1 Real-Time Quantitative Polymerase Chain Reaction (RT-qPCR)

RT-qPCR was used for the detection of cytokine expression at the mRNA level.

4.2.3.1.1 Spleen Processing and Isolation of Total RNA

Spleen samples were homogenized in RNA Blue (Top-Bio, Prague, Czech Republic) and total RNA was isolated according to the manufacturer's protocol. Total RNA was then used for one-step RT-qPCR using a SensiFAST™ SYBR® No-ROX One-Step Kit (Bioline, London, UK), according to manufacturer's protocol.

100 ul of chloroform was added to the samples of tissues homogenized in 0.5 ml of RNA Blue (Top-Bio) and vortexed for 30 seconds. After a 10-minute incubation period, the samples were centrifuged at 12,000 x g and 4°C for 15 minutes. The resulting supernatant was transferred and combined with 250 ul of isopropanol. Subsequently, the samples were incubated for 10 minutes at room temperature and then centrifuged at 13,500 x g and 4°C for 10 minutes. The supernatant was then decanted, and the pellet containing RNA was washed with 0.5 ml of 75% ethanol. The samples were centrifuged again for 10 minutes at 4°C and 13,500 x g. Upon removal of the supernatant, the RNA pellet was air-dried and resuspended in 50 ul of RNase-free water.

4.2.3.1.2 Determination of Cytokine Expression by One-Step RT-qPCR

One-step reverse transcription quantitative PCR (RT-qPCR) was performed using the kit SensiFAST SYBR No-ROX One-Step Kit (BioLine) according to the manufacturer's protocol in a total volume of 10 µl. Into the reaction mixture prepared according to the manufacturer's instructions (2.5 µl H2O, 5 µl 2x SensiFAST™ SYBR® No-ROX One-Step Mix, 0.1 µl reverse transcriptase and 0.2 µl RNase inhibitor (10 U/µl) per sample) were added respective primers at a final concentration of 200 nM. The primers used are shown in Table No 3. They were taken from the literature or designed using the Primer-BLAST program to detect only the spliced RNA. All primers were synthesized by Integrated DNA Technologies. RNA was freshly denatured before the use. RT-qPCR was performed using LightCyler LC480 (Roche) using the following conditions: reverse transcription 30 min at 45 °C, initial denaturation 5 min at 95 °C, 55 cycles of denaturation for 15 s at 95 °C, annealing and extension for 1 min at 60 °C, terminal extension for 10 min at 60 °C, and the melting curve analysis. The mean of technical duplicates was used for relative quantification of each target compared to GAPDH mRNA.

Selected the primers used:

Hu TNFa 71 L	5'-CTGCTGCACTTTGGAGTGAT-3'
Hu TNFa 71 R	5'-AGAGGGCTGATTAGAGAGAGGT-3'
Hu GAPDH 93_2 L	5'-CATGTTCGTCATGGGTGTGAAC-3'
Hu GAPDH 93_2 R	5'-AGGGGTGCTAAGCAGTTGGT-3'
Mu IFNγ L	5'-TGG CAT AGA TGT GGA AGA AAA GAG-3'
Mu IFNγ R	5'-TGC AGG ATT TTC ATG TCA CCA-3'
Mu IL-1β L	5'-TCC ATT GAG GTG GAG AGC TT-3'
Mu IL-1β R	5'-GGA TGA GGA CAT GAG CAC CT-3'
Mu iNOS L	5'-ACG AGA CGG ATA GGC AGA GA-3'
Mu iNOS R	5'-GCA CAT GCA AGG AAG GGA AC-3'
Mu IL-10 L	5'-AGG CGC TGT CAT CGA TTT CTC-3'
Mu IL-10 R	5'-GCC TTG TAG ACA CCT TGG TCT T-3'
Mu GAPDH L	5'-CGG TGC TGA GTA TGT CGT GGA -3'
Mu GAPDH R	5'- GGC AGA AGG GGC GGA GAT GA-3'
Mu TNFα L	5'- GAT CGG TCC CCA AAG GGA TG-3'
Mu TNFα R	5'- TGA GGG TCT GGG CCA TAG AA-3'

Table 1: Sequences of primers used.

4.2.3.2 Detection of Cytokines Using CBA (Cytokine Beads Assay)

The Legendplex Multi-Analyte Flow Assay Kit Mouse Anti-Virus Response Panel (Biolegend) - IL-12, IL-1β, IFN-α, IL-6, IL-10 and Legendplex Multi-Analyte Flow Assay Kit Mouse Th Cytokine Panel (12-plex) with Filter Plate V03 (Biolegend) – IFN-γ, TNF-α, IL-2, IL-4, IL-17A, IL-22 was used to detect cytokines in the plasma of infected and control mice. We used selected cytokines from the kits Mouse Anti-Virus Response Panel and Mouse Th Cytokine Panel. These kits employ beads with distinct fluorescence intensities and size each bound with antibodies against a specific cytokine. The cytokine and antibody interaction is then detected using a phycoerythrin (PE)-conjugated secondary antibody using flow cytometry.

To prepare the samples for analysis, we followed the manufacturer's protocol. The first step was to prepare a suspension of samples and beads specific for individual cytokines, using 10 µl of mixed beads per sample. We pipetted 10 µl of this mixture per sample. Then, we added 10 µl of the standards in the 4-fold dilution for the calibration curve. After incubating the samples and standards for 2 hours in the dark at room temperature, we centrifuged them and carefully aspirated the supernatant. Next, we added 80 ul of wash buffer (part of the kit) and centrifuged them at 250 g for 5 minutes at room temperature. After carefully aspirating the supernatant, we added 10 µl of Detection Antibodies and incubated them for 1 hour in the dark at room temperature. Subsequently, we added 10 µl of PE-conjugated detection antibody to the sample and standards and incubated them for 30 minutes in the dark at room temperature. The samples were then centrifuged at 250g for 5 minutes at room temperature, the supernatant removed, and 80 µl of wash buffer added. Following another 5-minute centrifugation at 250g at room temperature, the supernatant was discarded and 60 µl of wash buffer added before measuring in the flow cytometer FACSCanto™ II (Becton Dickinson) with 3 lasers emitting at 405, 488, and 633 nm, and with 8 detectors.

Cytometer setup was performed according to the kit protocol using calibration beads (Cytometer Setup Beads), and samples were analyzed in a PE-A x APC-A dot plot. The subsequent analysis was performed using The LEGENDplex™ Data Analysis Software Suite. The concentrations of individual analytes were determined by the SW-generated calibration curve.

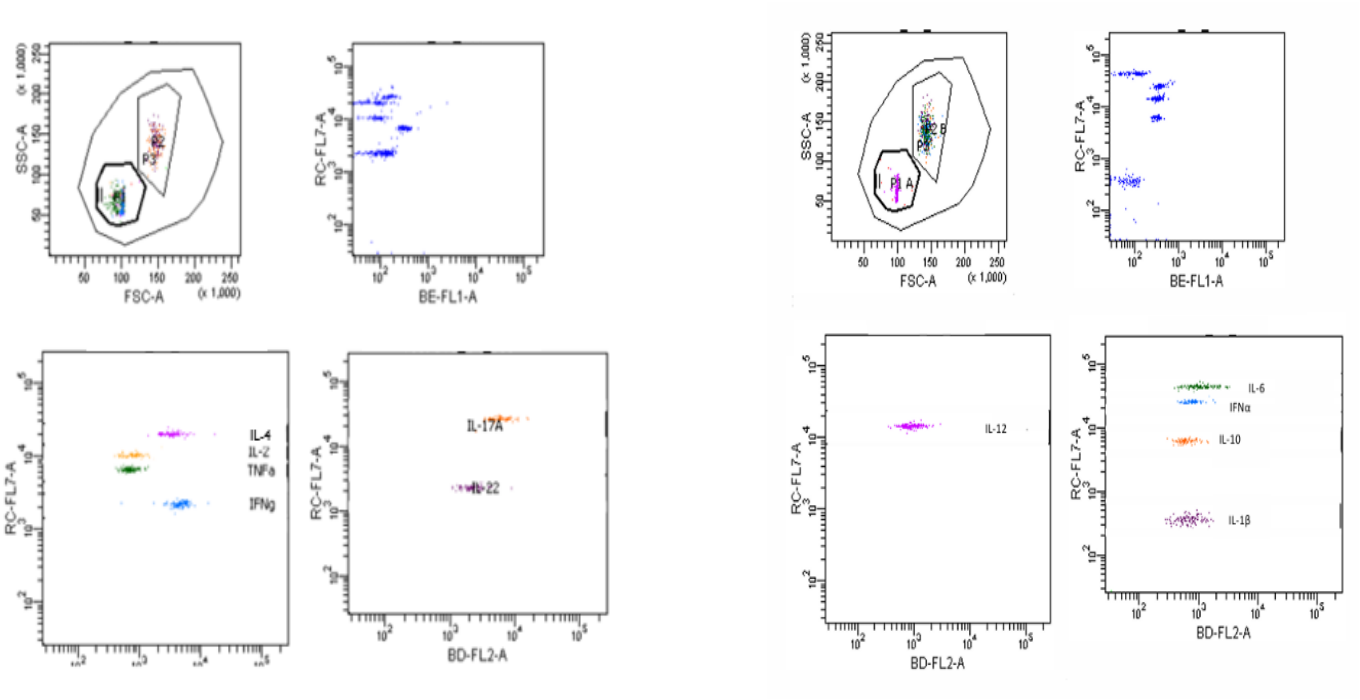

Figure 5: Gating Strategy

4.2.3.3 Histology

4.2.3.3.1 Tissue Processing

Lungs of infected and control mice were fixed with 4% paraformaldehyde in PBS in the Virology laboratory at the Institute of Immunology and Microbiology of the 1st Faculty of Medicine, Charles University, led by Dr. Mělková. The histology sections were then processed at the Vinicna Microscopy Core Facility, Faculty of Science, Charles University with the help of Mgr. Anna Maria Frontino, Mgr. Zuzana Brůhová and Mgr. Lenka Doubravská, Ph.D. In the Tissue Processor, Leica ASP200, samples undergo dehydration, clearing, and paraffin infiltration according to standard protocol (Table 2). Afterward, they were embedded in paraffin at the Leica Embedding Station.

1.	Ethanol 70%	1 hour
2.	Ethanol 100%	1 hour
3.	Ethanol 100%	1 hour
4.	Ethanol 100%	1 hour
5.	Ethanol 100%/Isopropanol (1:1)	1 hour
6.	Ethanol 100%/Isopropanol (1:1)	1 hour
7.	Xylene	1 hour
8.	Xylene	1 hour
9.	Xylene	1 hour
10.	Histowax	1,5 hour
11.	Histowax	2 hour
12.	Histowax	2 hour

Table 2 Tissue Processing Protocol

4.2.3.3.2 Staining

The deparaffinized sections were stained with hematoxylin and eosin (H&E) as summarized in Table 3. The staining of nuclei in blue and cytoplasm in pink with hematoxylin and eosin, respectively, enables visualization of cell morphology and inflammatory infiltrates. The sections were analyzed under an Olympus 1X71 microscope (40x1,6 magnification) and imaged with an Olympus DP70 with the help of Prof.Jan Černý.

1.	Xylene I	5 minutes
2.	Xylene II	5 minutes
3.	Ethanol %100	5 minutes
4.	Ethanol %96	5 minutes
5.	Ethanol %80	5 minutes
6.	Distilled Water	5 minutes
7.	Hematoxylin	3 minutes
8.	H2O+NaHCO3	30 sc.
9.	Eosin	3 minutes

Table 3 Tissue Staining Protocol

4.2.4 Statistical Analyses

Statistical analyses were performed using GraphPad Prism5, ANOVA, and two-tailed unpaired Student's t-tests, with statistical significance at * $p < 0.05$, ** $p < 0.01$, and *** $p < 0.001$. The graphs represent levels of individual cytokines or mRNA levels with indicated medians.

5 Results

5.1 Experiments on Cell Lines

5.1.1 Effects of Heme Arginate on SARS-CoV-2 Replication and Expression of TNF-α in Vero Cells

Vero cell line was used to examine the impact of HA on SARS-CoV-2 replication and TNFα expression at the mRNA level. The cells were infected with two different inocula of SARS-CoV-2, and treated with two different doses of HA. At 24 hours after infection, total RNA was isolated from the collected cells for RT-qPCR analysis, using GAPDH as a reference gene. As shown in Fig. 6, HA effectively inhibited virus growth in a dose-dependent manner at both levels of virus inoculum. Additionally, a decrease in the TNFα/GAPDH ratio was observed, as shown in Fig. 7.

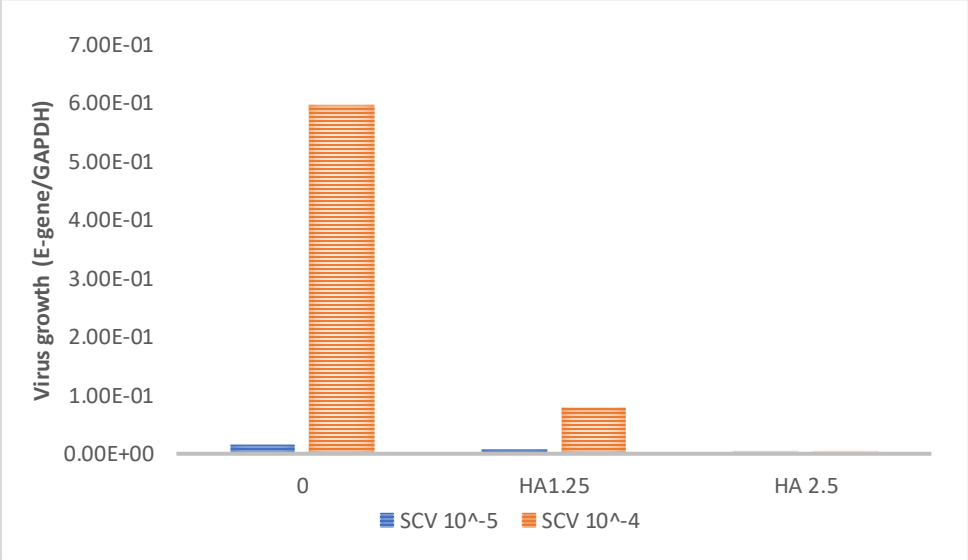

Figure 6: Effect of Heme Arginate on virus replication: Vero cells were infected with 2 dilutions (200 µl/sample of the 10^{-5} and 10^{-4} dilutions of the original stock) of SARS-CoV-2 and treated with two doses of HA (1.25 and 2.5µl/ml, i.e. final concentration of heme 48 and 96 µM, respectively). At 24h after infection, levels of SARS-CoV-2 E-gene RNA were quantified by RT-qPCR and normalized to GAPDH mRNA.

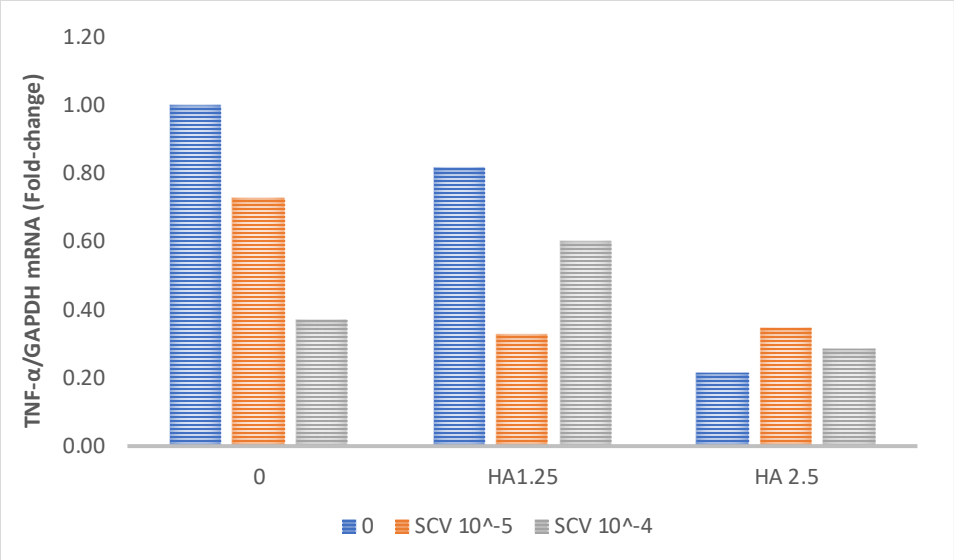

Figure 7: **Effect of Heme Arginate on TNF-α mRNA:** Vero cells were infected with 2 dilutions (200 µl/sample of the 10^{-5} and 10^{-4} dilutions of the original stock) of SARS-CoV-2 and treated with two doses of HA (1.25 and 2.5µl/ml, i.e. final concentration of heme 48 and 96 µM, respectively). At 24h after infection, levels of TNF-α mRNA were quantified by RT-qPCR and normalized to GAPDH mRNA.

5.2 Experiments in Mice

The experiments in mice were performed by Dr. Mělková and collaborators. As a mouse model, K18-hACE2 mice which express human ACE2 receptor under control of the human keratin 18 promoter, were used.

Male and female mice aged 7-10 months were divided into 5 groups. The control group consisted of uninfected mice, while remaining mice were intranasally administered SARS-CoV-2 (25 PFU/mouse in a volume of 10 µl, i.e. 5 ul/each nostril). Group 0 was infected but received only 1x PBS. The HA group was treated with Heme Arginate, the R group was treated with Remdesivir, and the HA+R group was treated with both Heme Arginate and Remdesivir.

After infection, PBS, HA and Remdesivir were administered at specific intervals and all the mice were sacrificed on day 4 post-infection.

5.2.1 Determination of Cytokine mRNA in the Spleens of Intranasally Infected Mice

The spleen is an important secondary lymphatic organ where several key processes essential for the induction of adaptive immune responses take place. Therefore, the mRNA levels of cytokines listed below were chosen to characterize.

Total RNA was isolated from the spleen homogenates in RNA Blue. The mRNA levels for TNF-α, IL-1β, IFN-γ, iNOS, and, IL-10 were determined by RT-qPCR and normalized to GAPDH mRNA.

There were different tendencies in male and female mice. In female mice, we observed only a few statistically significant differences among individual groups (Fig. 8). For IFN-γ mRNA, statistically significant differences were found in groups 0 and HA+R compared to the control group. Additionally for TNF-α mRNA, we found statistically significant differences between groups 0 and R. Nevertheless, HA treatment in general seemed to return the cytokine mRNA levels towards the levels found in control mice.

In male mice, we were unable to find any significant differences among individual groups (Fig. 9). Nevertheless, we noticed clear trends suggesting that HA treatment was decreasing the cytokine mRNA levels compared to group 0.

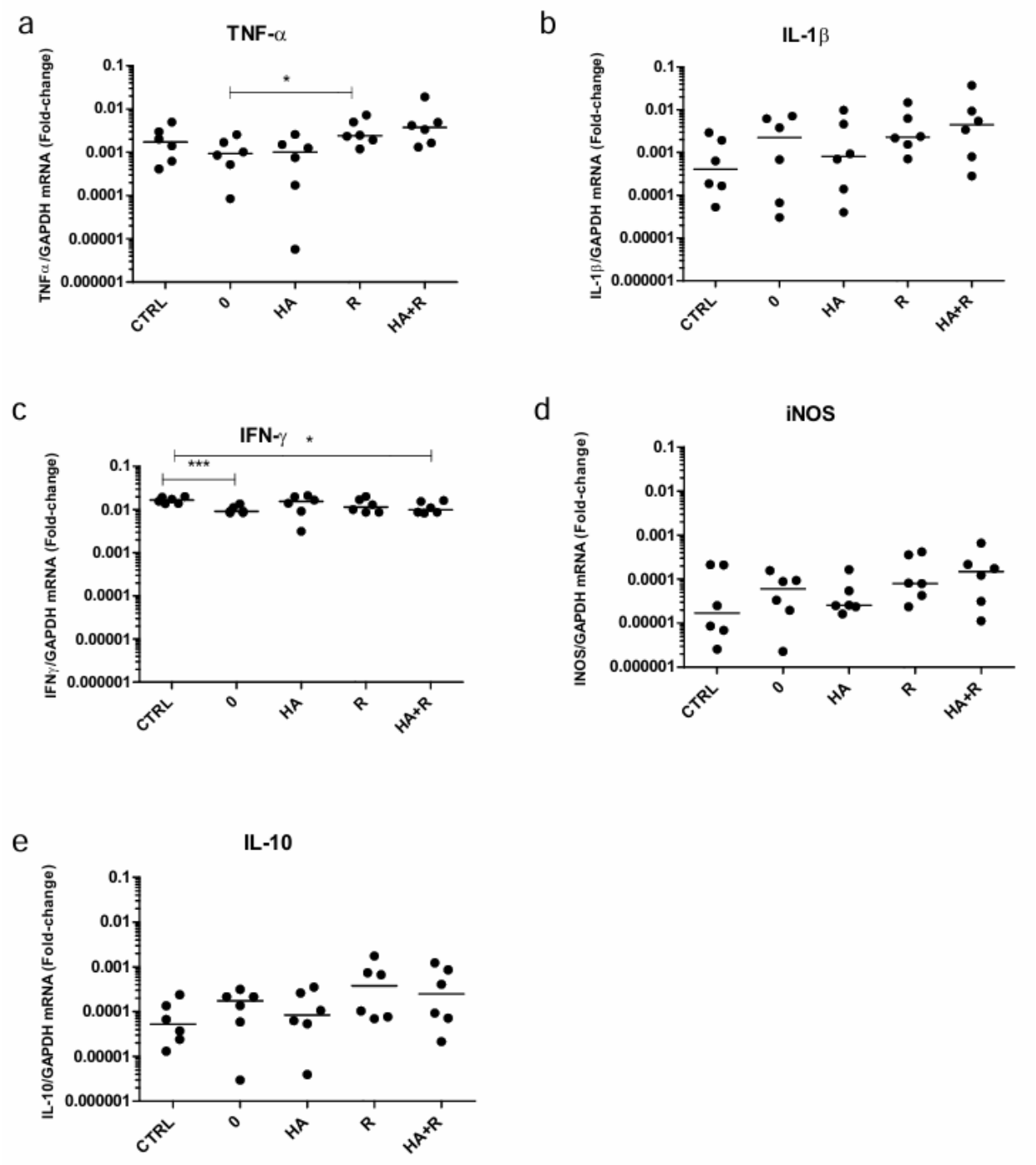

Figure 8: Expression of the cytokines and other factors at the mRNA level in spleens of female K18-hACE2 mice after intranasal inoculation with SARS-CoV-2. mRNA levels of each analyte were quantified by RT-qPCR and normalized to GAPDH mRNA. Statistical significance was determined by one-way ANOVA and t-test compared to the control and untreated groups. Data represent median of each group. N= 6 for each group. *P < 0.05, ***P < 0.001. (a) TNF-α, (b) IL-1β, (c) IFN-γ, (d) iNOS, (e) IL-10 mRNA.

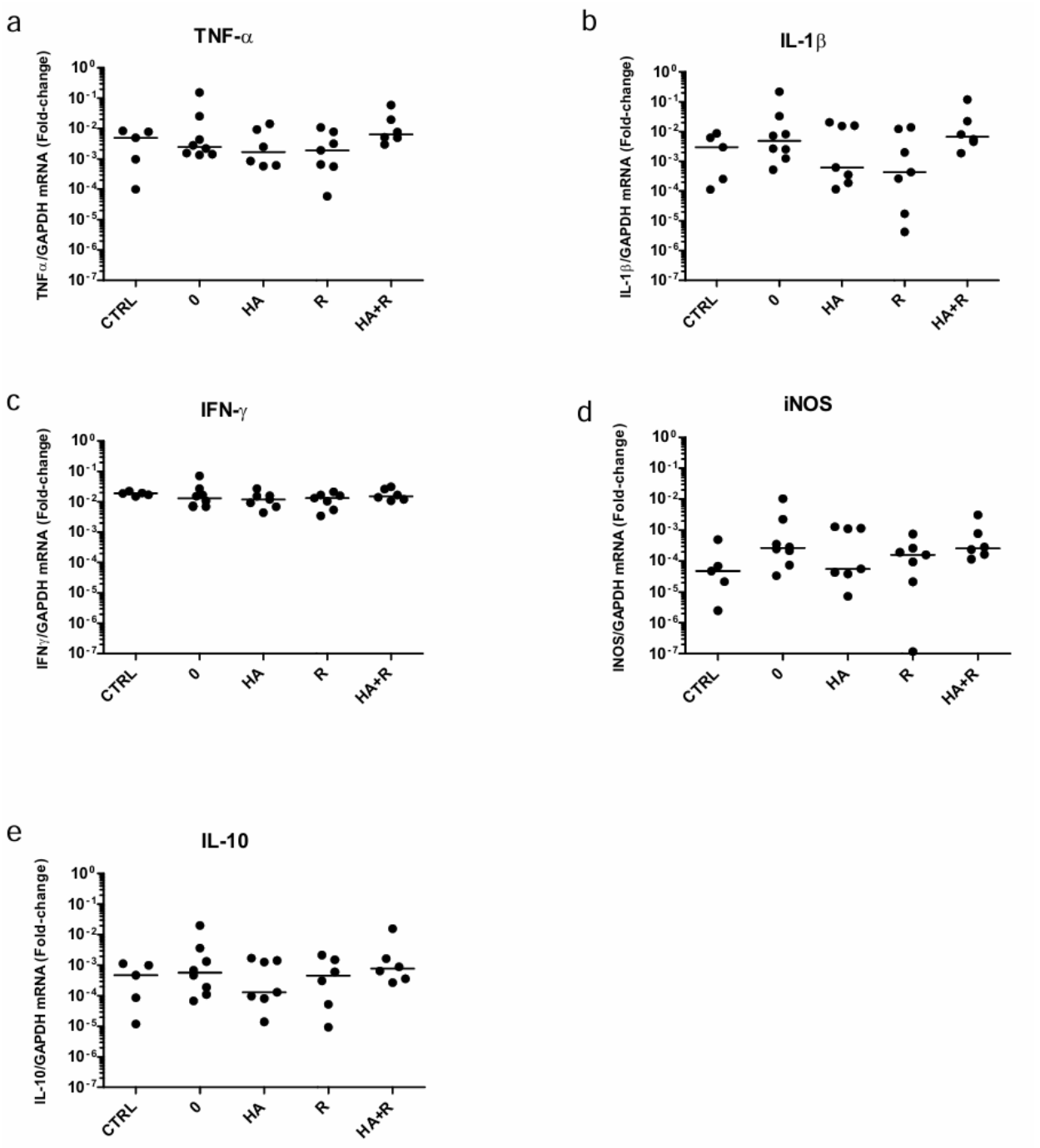

Figure 9: Expression of the cytokines and other factors at the mRNA level in spleens of male K18-hACE2 mice after intranasal inoculation with SARS-CoV-2. mRNA levels of each analyte were quantified by RT-qPCR and normalized to GAPDH mRNA. Statistical significance was determined by one-way ANOVA and t-test compared to the control and untreated groups. Data represent median of each group. N= 5, 8, 6, 7, and 6 for control, 0, HA, R, HA+R, respectively. P>0.05. (a) TNF-α, (b) IL-1β, (c) IFN-γ, (d) iNOS, (e) IL-10 mRNA.

5.2.2 Determination of Cytokine Levels in Mouse Plasma

To characterize cytokine levels in mouse plasma we used Cytokine Bead Assay (CBA). We have monitored IL-1β, IL-6, TNF-α, IFN-α, IFN-γ, IL-2, IL-17A, IL-12p70, IL-10, IL-4, IL-22.

There were different tendencies for male and female mice. At 4 days after infection for most cytokines in females (except for IL-1β and IL-6), there was a tendency to increase in the infected group 0 compared to the uninfected Ctrl group (Fig.10). For IFN-γ and IL-22, HA treatment tends to normalize the levels of these cytokines towards the levels found in control mice. On the other hand, HA increased the levels of TNF-α and IL-4 compared to group 0. In general, Remdesivir treatment did not seem to normalize the levels of most cytokines except of the significant decrease in IL-10. HA+R treatment revealed a tendency to decrease most cytokine levels.

For most cytokines in males (except for IL-22), there was a tendency to increase in the infected group 0 compared to the uninfected Ctrl group (Fig. 11). HA treatment tends to decrease the levels of cytokines compared to group 0, except for IFN-γ, IL-6, and IL-10. Remdesivir treatment seems to somewhat decrease the levels of TNF-α, IL-4, IL-22, IL-17, IFN-α, and significantly in IL-10. HA+R treatment revealed a tendency to decrease the levels of IL-2, IL-22, IL-17, IL-1b, IL-10, IFN-α and to increase levels of TNF-α, IFN-γ, and IL-4.

Calibration curves of individual cytokines are presented in Fig. 12.

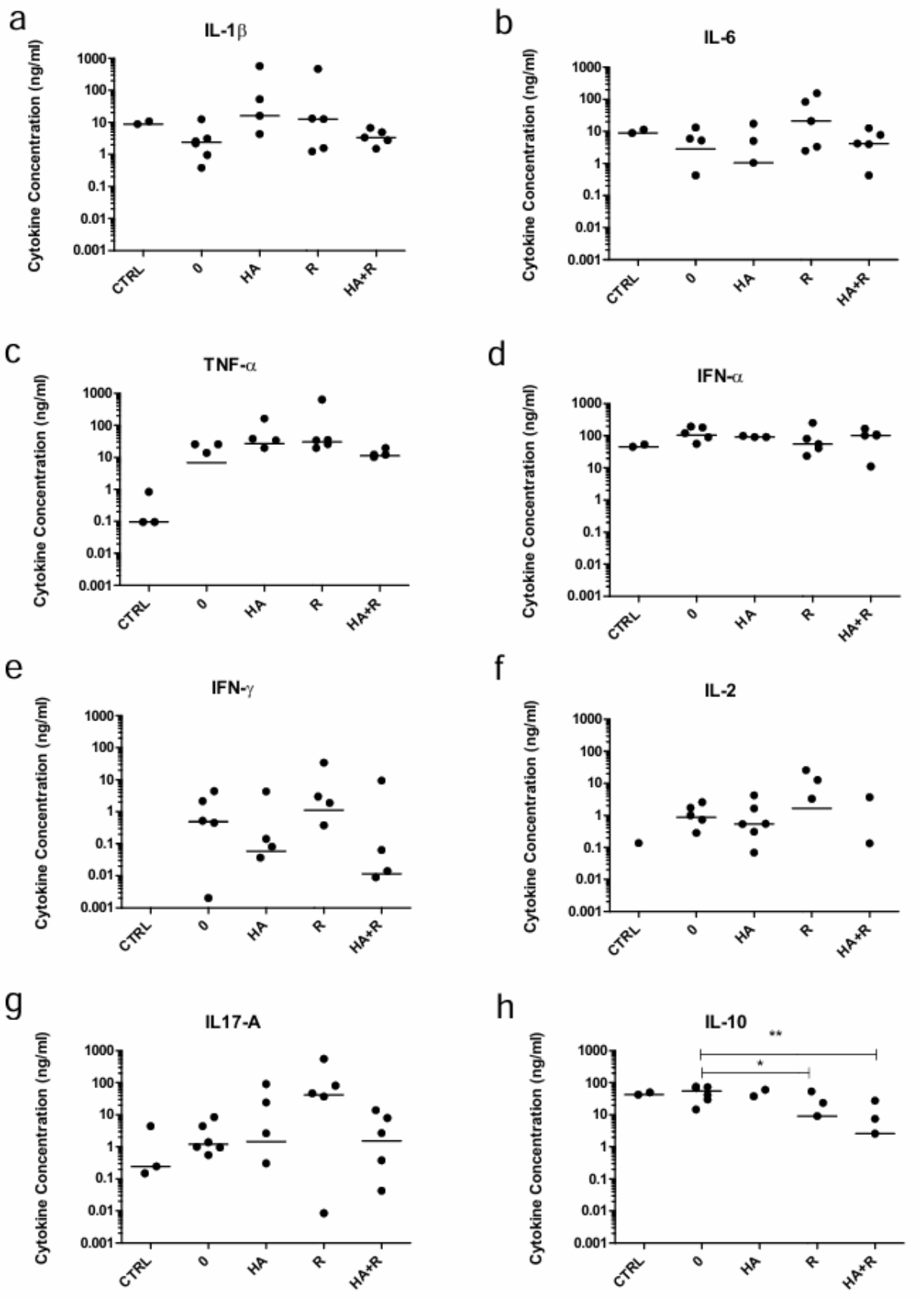
a
IL-1β
b
IL-6
c
TNF-α
d
IFN-α
e
IFN-γ
f
IL-2
g
IL17-A
h
IL-10
Cytokine Concentration (ng/ml)
1000
100
10
1
0.1
0.01
0.001
CTRL
0
HA
R
HA+R
**
*

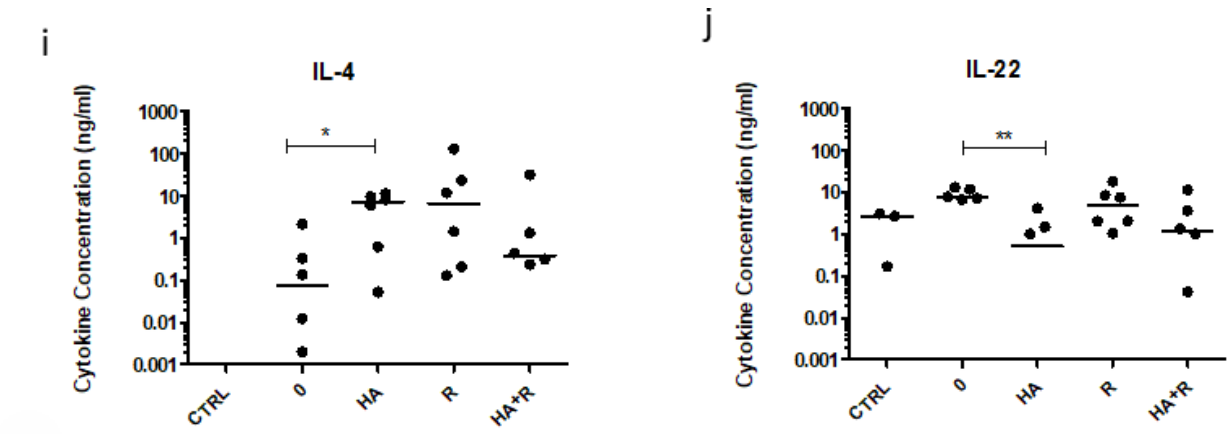

Figure 10: Levels of cytokines in plasma of female K18-hACE2 mice after intranasal inoculation with SARS-CoV-2. Cytokine levels of each mice were quantified by CBA. Statistical significance was determined by one-way ANOVA and t-test compared to the control and untreated groups. Data represent median of each group. Values equal to 0 are not indicated due to the logarithmic scale of the y-axis. N= 3, 6, 6, 6, 6 for control, 0, HA, R, HA+R, respectively. *P < 0.05**P < 0.01. (a) IL-1β, (b) IL-6, (c) TNFα, (d) IFN-α, (e) IFN-γ, (f) IL-2, (g) IL-17A, (h) IL-10, (i) IL-4, (j) IL-22.

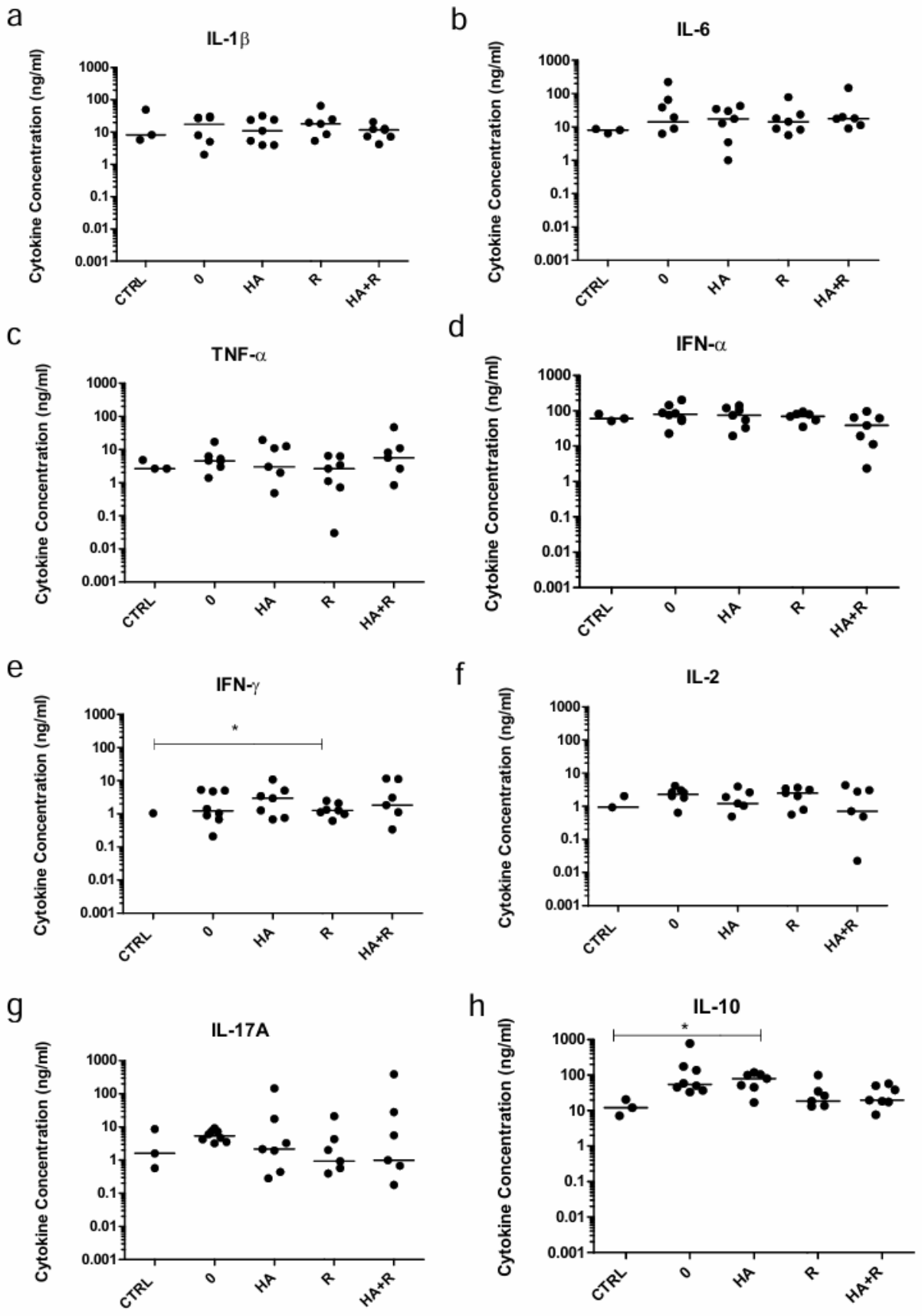
a
IL-1β
b
IL-6
c
TNF-α
d
IFN-α
e
IFN-γ
f
IL-2
g
IL-17A
h
IL-10
Cytokine Concentration (ng/ml)
1000
100
10
1
0.1
0.01
0.001
CTRL
0
HA
R
HA+R
*

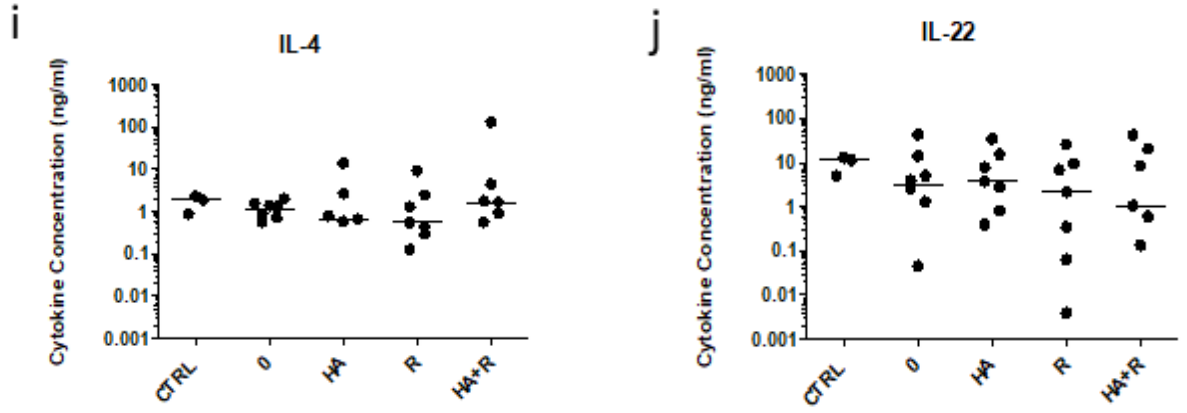

Figure 11: Expression of the cytokines in plasma of male K18-hACE2 mice after intranasal inoculation with SARS-CoV-2. Cytokines levels of each mice were quantified by CBA. Statistical significance was determined by one-way ANOVA and t-test compared to the control and untreated groups. Data represent median of each group. Values equal to 0 are not indicated due to the logarithmic scale of the y-axis. N= 3, 8, 7, 7, 7 for control, 0, HA, R, HA+R, respectively. **P < 0.01. (a) IL-1β, (b) IL-6, (c) TNF-α, (d) IFN-α, (e) IFN-γ, (f) IL-2, (g) IL-17A, (h) IL-10, (i) IL-4, (j) IL-22.

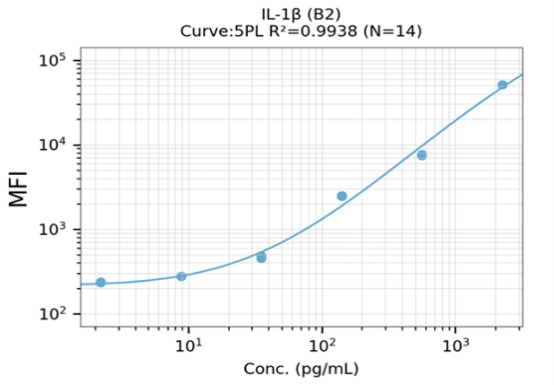
IL-1β (B2)
Curve:5PL R²=0.9938 (N=14)
MFI
Conc. (pg/mL)

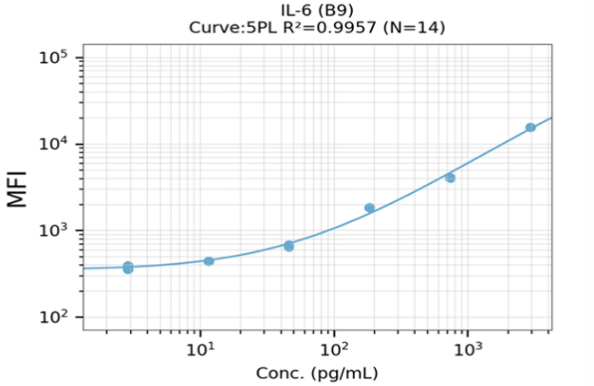
IL-6 (B9)
Curve:5PL R²=0.9957 (N=14)
MFI
Conc. (pg/mL)

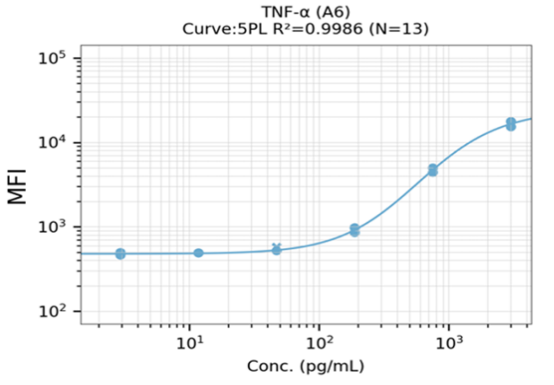
TNF-α (A6)
Curve:5PL R²=0.9986 (N=13)
MFI
Conc. (pg/mL)

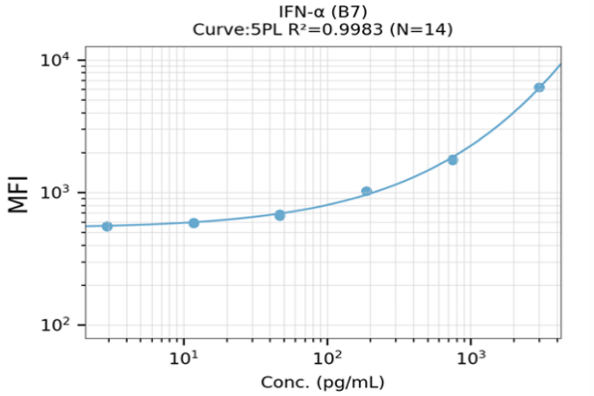
IFN-α (B7)
Curve:5PL R²=0.9983 (N=14)
MFI
Conc. (pg/mL)

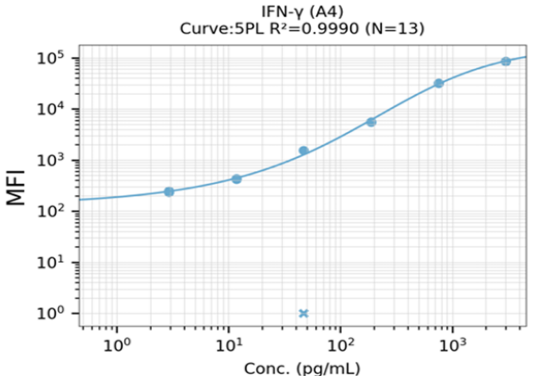
IFN-γ (A4)
Curve:5PL R²=0.9990 (N=13)
MFI
Conc. (pg/mL)

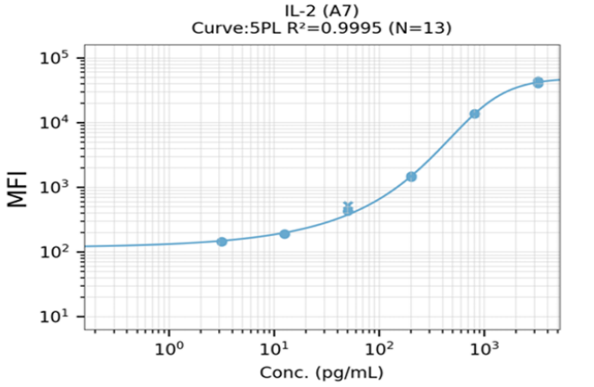
IL-2 (A7)
Curve:5PL R²=0.9995 (N=13)
MFI
Conc. (pg/mL)

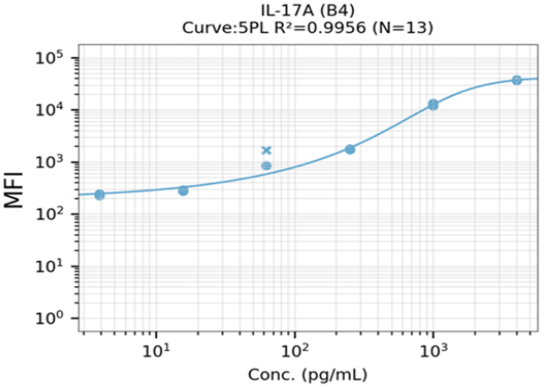
IL-17A (B4)
Curve:5PL R²=0.9956 (N=13)
MFI
Conc. (pg/mL)

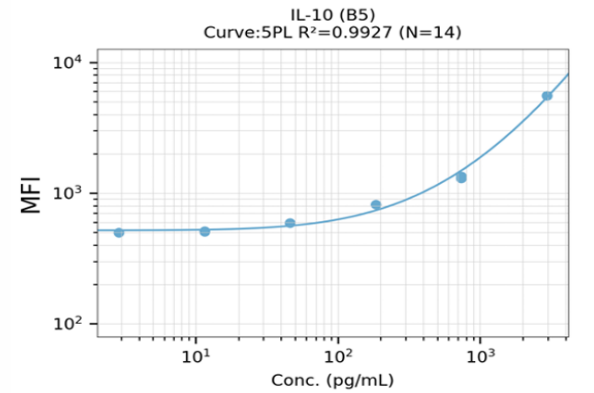
IL-10 (B5)
Curve:5PL R²=0.9927 (N=14)
MFI
Conc. (pg/mL)

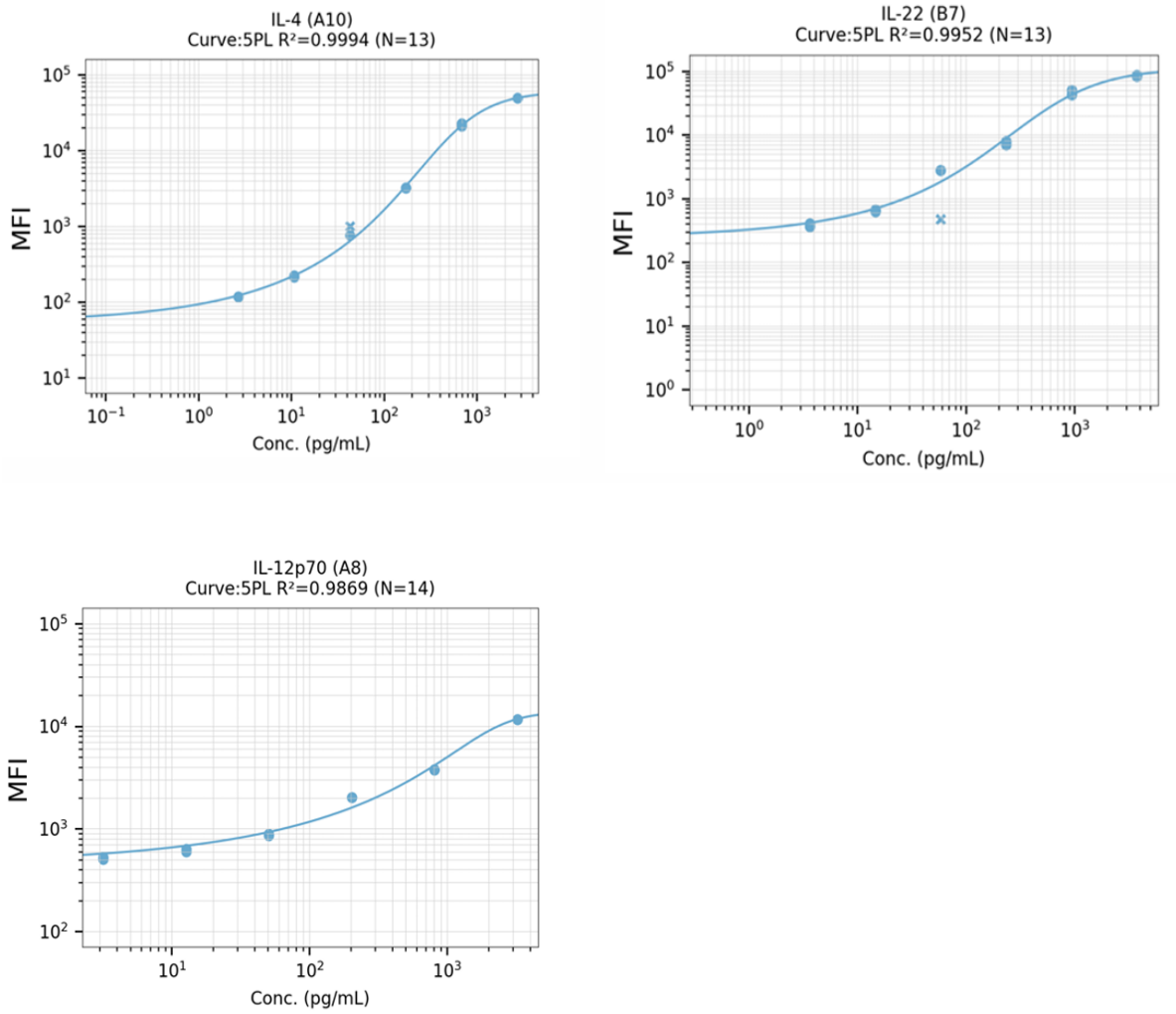

Figure 12: Calibration Curves for Individual Cytokines showing the relationship between the mean of fluorescence intensity (MFI) and concentration. Each data point represents the duplicate measurement.

5.2.3 Histology of Lungs

The histology of lung tissue was performed to observe morphological differences between the groups. Due to the spectral changes by the camera used, the sections are brownish. However, the original colors are purple and blue. The preliminary results showed that males lung tissue in group 0 and females lungs in the HA group revealed higher inflammatory infiltration. The lung parenchyma in males group 0 was also condensed. In the R and HA+R groups, both genders displayed similar characteristics.

Females		Males
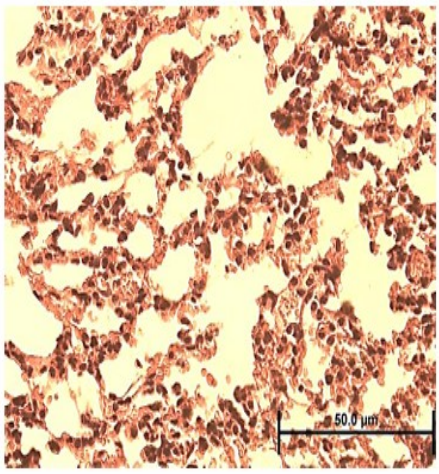	Control	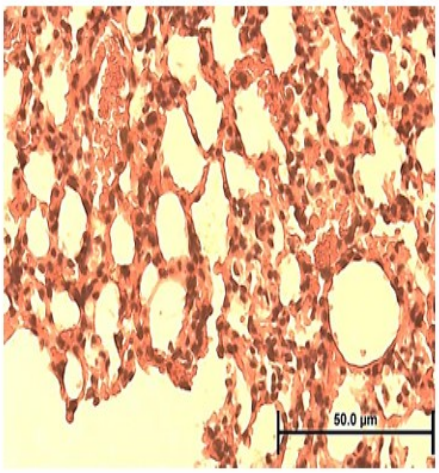
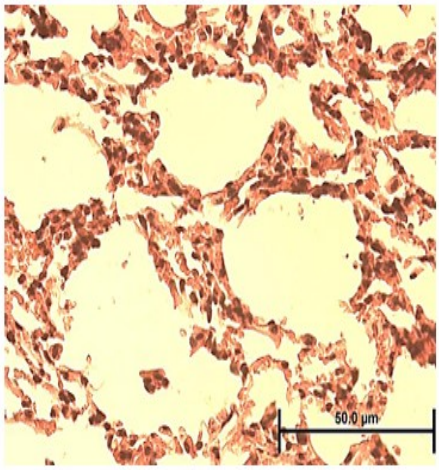	Group 0	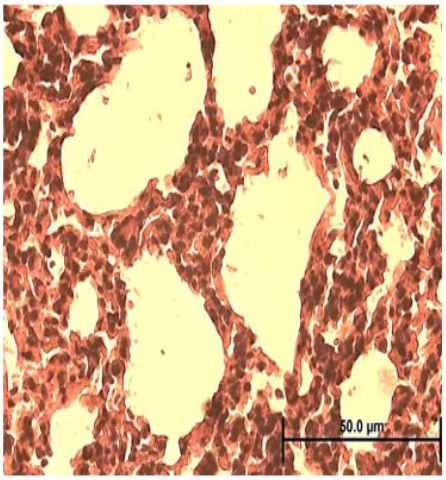

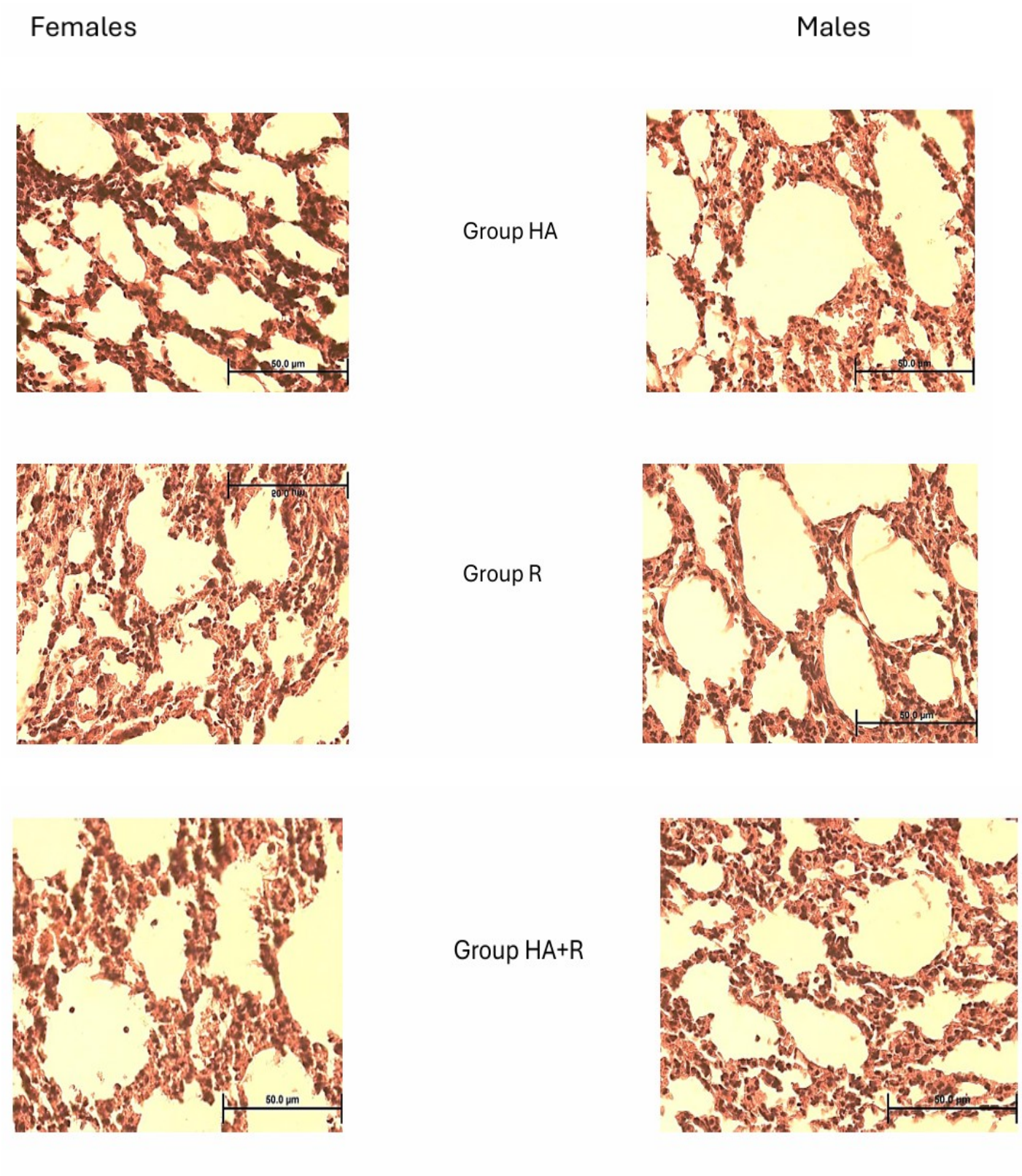

Figure 13: Histological section of lung tissue stained with H&E staining. Images were captured at 40x1,6 magnification and an Olympus DP70 camera.

6 Discussion

This thesis investigates the effects of heme arginate treatment on SARS-CoV-2 infection and its impacts on cytokine levels in a K18-hACE2 mouse model. Remdesivir treatment was used as a control to assess HA effectiveness. Characterization of primary immune responses against SARS-CoV-2 was performed based on the determination of mRNA and protein levels of several cytokines representing proinflammatory and anti-inflammatory groups. While plasma cytokine levels may not correspond to their actual local concentrations in the infected organs, mRNA levels do not directly correlate with the cytokine protein and/or function and can merely serve as markers of inflammatory elements that infiltrate the tissue analyzed.

The course of SARS-COV-2 infection in human reveals a wide range of symptomatology and severity. While the mild infection characterized namely by a common respiratory symptomatology resolves in about one week in most individuals, dysregulated immune responses result in the disease progression, worsening of the respiration, hospitalization and even death in some patients. Depending on the time of admission to the hospital since the disease onset, standard of care included namely antivirals, anti-inflammatory treatment (corticosteroids), and anticoagulants in addition to the oxygen therapy, hydration and possibly antibiotics. Lately, based on the new knowledge of the role of specific cytokines in COVID-19 pathogenesis, monoclonal antibodies against IL-6 receptor or inhibitors of JAK/STAT pathway were also used.

In contrast, our experiments in the mouse model of COVID-19, focused only on the effects of heme arginate and remdesivir. In the laboratory of Dr. Mělková, using the K18-hACE2 mice the effects of HA on virus replication and survival differed based on the way of infection (intranasal versus intrapulmonary), time and number of applications, and the gender of the mice. Based on the preliminary results, the time of administration of HA was set to 2 days p.i., with the end of experiment at 4 days p.i.

In this work, we characterized the effect of HA and R in mice infected intranasally, which corresponds better to the natural course of infection in human. The virus RNA levels were determined in various organs, namely lungs, brain, and kidneys. There were saddle changes in virus levels in lungs and brains, the organs preferentially infected upon the intranasal infection. In males, there was a tendency to lower or no detection of SARS-CoV-2 in kidneys in all HA, R,

and HA+R groups. In females this trend was not observed and further analyses are required (Dr. Mělková, unpublished results).

In my work, I focused on the characterization of cytokine changes in spleen and plasma of these mice at the mRNA and protein levels, respectively. IL-1β, IL-6, TNF-α, and IFN-γ were chosen as cytokines important for the type of differentiation of and signature cytokine production by T-cells. The individual types of responses were characterized by selected cytokines. For Th1 responses IFN-γ and IL-12, for Th2 IL-2 and IL-4, for Th17 IL-6, IL-17, and IL-22, and for Th22 IL-6, IL-1β, and IL-22 were chosen. To address the resolution phase of the inflammation, we chose IL-10. Finally, IFN-α as the primary antiviral interferon that might indicate the continuous replication of the virus was determined.

Unfortunately, in most cases, no statistically significant differences were found. Thus, only trends in changes of individual cytokines and their correlation with cytokines expressed in human are discussed.

Recent studies have found that TNF-α is upregulated in acute lung injury caused by SARS-CoV-2, leading to CRS and facilitating the virus interaction with hACE2 (Guo et al., 2022). It is supposed that upregulation of TNF-α by SARS-CoV-2 infection causes mitochondrial damage and higher production of ROS with the resulting negative effects on the antiviral responses (Anwar et al., 2022). The generation of ROS can be neutralized by the action of HO-1, the primary enzyme induced by heme and/or HA, that reveals protective effects against oxidative stress and affects various immune responses (Martínez-Casales et al., 2021). Our first aim was to determine the impact of HA on SARS-CoV-2 replication and to characterize the production of TNF-α in infected Vero cells. In these cells, HA was able to dose-dependently inhibit virus growth upon infection with two different dilutions of SARS-CoV-2; simultaneously, HA decreased TNF-α mRNA levels as well. However in vivo, we found no decrease in TNF-α levels in response to HA in mRNA and protein levels in spleen or plasma, respectively. On the contrary, HA+R seemed to increase the levels of this cytokine. Nevertheless, due to different outcomes of TNF-α signaling through its different receptors, it is impossible to conclude if such an effect is harmful or might be beneficial.

During SARS-CoV-2 infection, CD4+ and CD8+ T lymphocytes, as well as IFN-γ levels were found decreased (Montazersaheb et al., 2022). Several studies have shown that IFN-γ stimulated macrophages to release ROS and polarized them to the M1 phenotype while suppressing the M2 pathway. This activation leads to the production of pro-inflammatory cytokines such as IL-12, TNF-α, and IL-1β (Lee & Ashkar, 2018). Study by (Karki et al., 2021) showed that the interaction between IFN-γ and TNF-α plays a crucial role in initiating massive inflammatory cell death, known as PANoptosis, through the JAK/STAT1/IRF1 pathway activation, induction of iNOS expression, and production of nitric oxide. The kinetics of the cell death induced by TNF-α and IFN-γ co-stimulation are proportional to their concentrations (Guo et al., 2022). In contrast, we have observed a correlation of plasma concentrations of IFN-γ with IL-1β and TNF-α in the individual mice of both genders, with IFN-γ decrease leading to an increase in TNF-α and IL-1β levels. The trend was found similar also in spleens at the level of mRNA (additional analyses not presented in this thesis).

IFN-γ mRNA levels in the female spleens revealed a significant decrease in the groups 0 and HA+R compared to the control group, while HA and R treatments seemed to keep the levels in the range of the control group. In male spleens, no differences among the individual groups were observed.

In plasma of both male and female mice, SARS-CoV-2 infection led to the increase of IFN-γ compared to control mice. In females, both HA and HA+R treatments tended to decrease IFN-γ levels while R treatment increased the levels compared to group 0. However, in males, all treatments tended to increase IFN-γ levels compared to the both control and 0 groups. In the same time, the virus RNA levels in lungs were about 10-fold lower in females, possibly allowing a better response to the treatments. Thus, the decrease in IFN-γ levels after HA could suggest a better antiviral response in females. On the other hand, increased levels of IFN-γ after HA in males might correspond to a different response upon higher infection.

As mentioned above, patients with severe and critical COVID-19 have a weakened IFN response, leading to low levels of IFN-α and IFN-β as well as to a decreased expression of ISGs (Hojun Choi, 2021). Accordingly in mouse plasma of both genders, IFN-α levels in the infected mice were almost comparable to the control mice. Further, none of the three differently treated groups displayed a significant difference compared to the control or 0 groups.

IL-12 is another key cytokine involved in the antiviral responses. According to the work of Tjan (Tjan et al., 2021), IL-12 and IL-2 levels are higher in patients with asymptomatic and mild COVID-19 compared to the moderate and severe conditions. In our experiments, we did not find any measurable levels of IL-12 at 4 days p.i. By analogy to human, it is possible to assume that the course of infection in the mice was relatively severe, as their survival was about 6-8 days in parallel experiments (Dr. Mělková et al., unpublished results).

On the other hand, other researchers reported that higher levels of IL-2 are directly related to the severity of the disease in human patients (Costela-Ruiz et al., 2020). In mice, an increase in IL-2 levels could be observed in infected mice of both genders, with a relatively higher difference found in females. In both genders, IL-2 concentrations, tended to decrease in HA and HA+R groups towards the level determined in the control group.

To make the story even more complicated, a meta-analysis study by Chang has mentioned that IL-1β, IL-2, and IL-4 levels are not related to the disease severity at all and another meta-analysis study done by Matuszewskı highlighted that the IL-4 levels were the lowest in both severe and mild COVID-19 groups compared to other cytokine concentrations (Chang et al., 2022; MATUSZEWSKI et al., 2022). In our experiments, IL-4 plasma levels in the infected mice were found in the lowest range of concentrations determined for other cytokines. In females, IL-4 levels were increased in the infected group 0 compared to control group, and all treatments further increased them. Only HA caused a statistically significant increase, though. In males, IL-4 levels were almost comparable between the infected and control mice, with HA+R being somewhat higher.

Research done by Oladunni in K18-hACE2 mice found that IL-1β production was absent at day 2 and 4 p.i. They mention that in human IL-1β precedes the other cytokines production. Thus a similar course of IL-1β production might occur in K18-hACE2 mice as well (Oladunni et al., 2020).

IL-1β mRNA levels in the female spleens revealed an increase in all groups compared to a control group. In male spleens, group 0 and HA+R were almost comparable to the control group while HA and R groups revealed a decrease compared to 0.

In plasma of infected female mice, IL-1β levels were somewhat decreased compared to controls. HA and R groups revealed an increase compared to 0, while HA+R, remained comparable to 0. In male plasma, we have not observed any major differences between the infected and control groups. Thus, our findings could correspond to finding of Oladunni, and IL-1β should be analyzed at an earlier time interval.

In individuals with SARS-CoV-2, IL-6 levels increase in both circulating monocytes and bronchoalveolar lavage fluid and elevate with disease severity as infected respiratory epithelial cells in the lungs release IL-6 as well. Accordingly, high levels of IL-6 correlate with a higher viral load (Mazzocco et al., 2023).

At 4 days p.i. in female mice, IL-6 levels were found decreased compared to control group and HA treatment tended to decrease its levels even further. In males, we observed a saddle increase in all infected mice compared to the control group.

Activation of the IL-17A signaling pathway in patients can be a therapeutic indicator for reducing complications, especially pulmonary ones, in those with COVID-19. It is also linked to the severity of viral respiratory infections and inflammatory side effects (Hasanvand, 2022). In both genders of mice, we observed and increase in IL-17A levels in group 0 compared to controls. In females, HA did not seem to affect the IL-17A levels, while R treatment seemed to increase them. In contrast in males, all treatments revealed a tendency to decrease IL-17A levels compared to group 0.

It was previously found that IL-22 does not lower virus levels but can alleviate pneumonia severity by regulating the immune system and providing protective functions to tissues. It also has antiviral and antibacterial properties against respiratory syncytial virus, which may be effective in managing SARS-CoV-2 infection (Fang et al., 2022). In females, IL-22 levels were increased in 0 compared to control group, with HA causing a significant decrease compared to 0. HA+R revealed a similar tendency. In males, all the infected groups revealed lower levels of IL-22 compared to the control group.

It has been found that HO-1 protects the lungs from inflammation and oxidative stress. It is beneficial in treating ALI and ARDS by increasing the levels of anti-inflammatory cytokines such as IL-10 (Toro et al., 2022). In our experiments, different tendencies in changes of IL-10

were found in spleen mRNA and plasma concentrations at 4 days p.i. In female but not male spleens, IL-10 mRNA levels were found increased in group 0 compared to controls. In both genders, HA treatment tended to decrease IL-10 mRNA levels compared to 0. The R and HA+R treatments revealed an increase in females, while no changes compared to group 0 were found in males.

In plasma, IL-10 levels were in contrast to mRNA in spleens increased in infected males compared to controls, but not in females. In females, all the treatments decreased the IL-10 levels compared to group 0, R, and HA+R significantly. In males, HA treatment revealed a saddle increase compared to 0, while R and HA+R tended to a decrease.

To complement the cytokine analyses, we have performed histology of the lungs. Based on the preliminary assessment of the hematoxylin&eosin-stained sections, in the selected infected female lung section, no major changes in the structure of lung parenchyma compared to control mice were observed. Unexpectedly, HA treatment seemed to increase the inflammatory infiltration of the lungs. In the selected infected male lung specimen, increased inflammatory infiltration and lung tissue condensation could be observed compared to the control one, possibly corresponding to the higher virus titers found in male lungs. The inflammatory changes then seemed to improve after HA treatment. In the lung sections of groups R and HA+R, the histology findings seemed similar in female and male tissues with no major differences compared to control sections. Thus, on the microscopic level, both R and HA+R treatments seem to be beneficial.

In this work, only one-time point p.i. was analyzed, while cytokine production and other immune responses develop and change with the time p.i. At 4 days p.i., early cytokines should be already down-regulated, while others may not be fully expressed yet. In some cytokines, the changes in the infected mice compared to controls were unexpected or did not seem to follow the established pattern. Even though the control mice were kept in the positive pressure and SPF conditions, it is not possible to exclude a possibility that their cytokine levels were not exactly normal. In general, HA+R treatment was more effective than HA treatment alone. On the other hand, R alone often did not cause any changes in cytokine levels; thus, combination HA+R might be more effective than R alone. Upon analysis of the levels of individual cytokines, it seems difficult to distinguish whether the effect observed is due to lower virus replication or due

to a direct effect of the treatment. In the early phases of infection, inhibition of virus replication is desirable, while at later times p.i., inhibition of excessive immune responses, that could potentially result in the lung and other tissue damage, is beneficial. Importantly though, compromised immune responses would be counterproductive in early stages.

In this work, the effect of HA treatment in a mouse model of COVID-19 was examined. Even though it provides new data about specific aspects of HA action on virus infection and pathogenesis, it is critical to emphasize that this model may not directly recapitulate the human condition. Also, mouse immune responses often differ from the human ones. On the other hand, the differences between the genders seem to be similar to human. In any case, the results presented in this thesis should be considered as preliminary as further analyses and possibly different experimental setup are required.

7 Summary

This work aimed to characterize the effect of Heme Arginate treatment on selected cytokines produced in response to SARS-CoV-2 infection, namely on levels of IL-1β, IL-6, TNF-α, IFN-α, IFN-γ, IL-2, IL-17A, IL-12p70, IL-10, IL-4, IL-22.

- In Vero cell line, HA inhibited virus growth in a dose-dependent manner at two different virus inocula.
- In Vero cell line, HA decreased TNFα/GAPDH ratio.
- In K18-hACE2 mice, HA induced changes in levels of the cytokines tested. The effect of HA+R was mostly higher than the effect of HA alone.
- In histology sections of the lung parenchyma, inflammatory infiltration and tissue condensation seemed to be ameliorated by HA+R.

8 References

Abulsoud, A. I., El-Husseiny, H. M., El-Husseiny, A. A., El-Mahdy, H. A., Ismail, A., Elkhawaga, S. Y., Khidr, E. G., Fathi, D., Mady, E. A., Najda, A., Algahtani, M., Theyab, A., Alsharif, K. F., Albrakati, A., Bayram, R., Abdel-Daim, M. M., & Doghish, A. S. (2023). Mutations in SARS-CoV-2: Insights on structure, variants, vaccines, and biomedical interventions. *Biomedicine & Pharmacotherapy*, *157*, 113977. https://doi.org/10.1016/j.biopha.2022.113977

Albayrak, N., Orte Cano, C., Karimi, S., Dogahe, D., Van Praet, A., Godefroid, A., Del Marmol, V., Grimaldi, D., Bondue, B., Van Vooren, J.-P., Mascart, F., & Corbière, V. (2022). Distinct Expression Patterns of Interleukin-22 Receptor 1 on Blood Hematopoietic Cells in SARS-CoV-2 Infection. *Frontiers in Immunology*, *13*, 769839. https://doi.org/10.3389/fimmu.2022.769839

Anwar, M. M., Sah, R., Shrestha, S., Ozaki, A., Roy, N., Fathah, Z., & Rodriguez-Morales, A. J. (2022). Disengaging the COVID-19 Clutch as a Discerning Eye Over the Inflammatory Circuit During SARS-CoV-2 Infection. *Inflammation*, *45*(5), 1875–1894. https://doi.org/10.1007/s10753-022-01674-5

Bakhiet, M., & Taurin, S. (2021). SARS-CoV-2: Targeted managements and vaccine development. *Cytokine & Growth Factor Reviews*, *58*, 16–29. https://doi.org/10.1016/j.cytogfr.2020.11.001

Barreto-Vieira, D. F., da Silva, M. A. N., de Almeida, A. L. T., Rasinhas, A. da C., Monteiro, M. E., Miranda, M. D., Motta, F. C., Siqueira, M. M., Girard-Dias, W., Archanjo, B. S., Bozza, P. T., L. Souza, T. M., Gomes Dias, S. S., Soares, V. C., & Barth, O. M. (2022). SARS-CoV-2: Ultrastructural Characterization of Morphogenesis in an In Vitro System. *Viruses*, *14*(2), Article 2. https://doi.org/10.3390/v14020201

Boraschi, D., Italiani, P., Weil, S., & Martin, M. U. (2018). The family of the interleukin-1 receptors. *Immunological Reviews*, *281*(1), 197–232. https://doi.org/10.1111/imr.12606

Brant, A. C., Tian, W., Majerciak, V., Yang, W., & Zheng, Z.-M. (2021). SARS-CoV-2: From its discovery to genome structure, transcription, and replication. *Cell & Bioscience*, *11*(1), 136. https://doi.org/10.1186/s13578-021-00643-z

Chang, Y., Bai, M., & You, Q. (2022). Associations between Serum Interleukins (IL-1β, IL-2, IL-4, IL-6, IL-8, and IL-10) and Disease Severity of COVID-19: A Systematic Review and Meta-Analysis. *BioMed Research International*, *2022*, 2755246. https://doi.org/10.1155/2022/2755246

Choi, H., & Shin, E.-C. (2021). Roles of Type I and III Interferons in COVID-19. *Yonsei Medical Journal*, *62*(5), 381–390. https://doi.org/10.3349/ymj.2021.62.5.381

Costela-Ruiz, V. J., Illescas-Montes, R., Puerta-Puerta, J. M., Ruiz, C., & Melguizo-Rodríguez, L. (2020). SARS-CoV-2 infection: The role of cytokines in COVID-19 disease. *Cytokine & Growth Factor Reviews*, *54*, 62–75. https://doi.org/10.1016/j.cytogfr.2020.06.001

Das, S., & Khader, S. (2017). Yin and yang of interleukin-17 in host immunity to infection. *F1000Research*, *6*, 741. https://doi.org/10.12688/f1000research.10862.1

Ding, H., Wang, G., Yu, Z., Sun, H., & Wang, L. (2022). Role of interferon-gamma (IFN-γ) and IFN-γ receptor 1/2 (IFNγR1/2) in regulation of immunity, infection, and cancer development: IFN-γ-dependent or independent pathway. *Biomedicine & Pharmacotherapy = Biomedecine & Pharmacotherapie*, *155*, 113683. https://doi.org/10.1016/j.biopha.2022.113683

Fang, S., Ju, D., Lin, Y., & Chen, W. (2022). The role of interleukin-22 in lung health and its therapeutic potential for COVID-19. *Frontiers in Immunology*, *13*. https://doi.org/10.3389/fimmu.2022.951107

Ghanbari Naeini, L., Abbasi, L., Karimi, F., Kokabian, P., Abdi Abyaneh, F., & Naderi, D. (2023). The Important Role of Interleukin-2 in COVID-19. *Journal of Immunology Research*, *2023*, e7097329. https://doi.org/10.1155/2023/7097329

Guimarães, L. M. F., Rossini, C. V. T., & Lameu, C. (2021). Implications of SARS-Cov-2 infection on eNOS and iNOS activity: Consequences for the respiratory and vascular systems. *Nitric Oxide*, *111*, 64–71. https://doi.org/10.1016/j.niox.2021.04.003

Guo, Y., Hu, K., Li, Y., Lu, C., Ling, K., Cai, C., Wang, W., & Ye, D. (2022). Targeting TNF-α for COVID-19: Recent Advanced and Controversies. *Frontiers in Public Health*, *10*. https://www.frontiersin.org/articles/10.3389/fpubh.2022.833967

Gusev, E., Sarapultsev, A., Solomatina, L., & Chereshnev, V. (2022). SARS-CoV-2-Specific Immune Response and the Pathogenesis of COVID-19. *International Journal of Molecular Sciences*, *23*(3), 1716. https://doi.org/10.3390/ijms23031716

Hamza, T., Barnett, J. B., & Li, B. (2010). Interleukin 12 a Key Immunoregulatory Cytokine in Infection Applications. *International Journal of Molecular Sciences*, *11*(3), 789–806. https://doi.org/10.3390/ijms11030789

Hasanvand, A. (2022). COVID-19 and the role of cytokines in this disease. *Inflammopharmacology*, *30*(3), 789–798. https://doi.org/10.1007/s10787-022-00992-2

Holbrook, J., Lara-Reyna, S., Jarosz-Griffiths, H., & McDermott, M. F. (2019). Tumour necrosis factor signalling in health and disease. *F1000Research*, *8*, F1000 Faculty Rev-111. https://doi.org/10.12688/f1000research.17023.1

Ivashkiv, L. B., & Donlin, L. T. (2014). Regulation of type I interferon responses. *Nature Reviews. Immunology*, *14*(1), 36–49. https://doi.org/10.1038/nri3581

Ju, X., Zhu, Y., Wang, Y., Li, J., Zhang, J., Gong, M., Ren, W., Li, S., Zhong, J., Zhang, L., Zhang, Q. C., Zhang, R., & Ding, Q. (2021). A novel cell culture system modeling the SARS-CoV-2 life cycle. *PLoS Pathogens*, *17*(3), e1009439. https://doi.org/10.1371/journal.ppat.1009439

Karki, R., Sharma, B. R., Tuladhar, S., Williams, E. P., Zalduondo, L., Samir, P., Zheng, M., Sundaram, B., Banoth, B., Malireddi, R. K. S., Schreiner, P., Neale, G., Vogel, P., Webby, R., Jonsson, C. B., & Kanneganti, T.-D. (2021). Synergism of TNF-α and IFN-γ Triggers Inflammatory Cell Death, Tissue Damage, and Mortality in SARS-CoV-2 Infection and Cytokine Shock Syndromes. *Cell*, *184*(1), 149-168.e17. https://doi.org/10.1016/j.cell.2020.11.025

Kawasaki, T., & Kawai, T. (2014). Toll-Like Receptor Signaling Pathways. *Frontiers in Immunology*, *5*, 461. https://doi.org/10.3389/fimmu.2014.00461

Lazear, H. M., Schoggins, J. W., & Diamond, M. S. (2019). Shared and Distinct Functions of Type I and Type III Interferons. *Immunity*, *50*(4), 907–923. https://doi.org/10.1016/j.immuni.2019.03.025

Lee, A. J., & Ashkar, A. A. (2018). The Dual Nature of Type I and Type II Interferons. *Frontiers in Immunology*, *9*, 2061. https://doi.org/10.3389/fimmu.2018.02061

Liang, Y., Fisher, J., Gonzales, C., Trent, B., Card, G., Sun, J., Tumanov, A. V., & Soong, L. (2022). Distinct Role of TNFR1 and TNFR2 in Protective Immunity Against Orientia tsutsugamushi Infection in Mice. *Frontiers in Immunology*, *13*. https://doi.org/10.3389/fimmu.2022.867924

Manohar, S. M. (2024). At the Crossroads of TNF α Signaling and Cancer. *Current Molecular Pharmacology*, *17*(1), e060923220758. https://doi.org/10.2174/1874467217666230908111754

Marston, J. L., Greenig, M., Singh, M., Bendall, M. L., Duarte, R. R. R., Feschotte, C., Iñiguez, L. P., & Nixon, D. F. (n.d.). SARS-CoV-2 infection mediates differential expression of human endogenous retroviruses and long interspersed nuclear elements. *JCI Insight*, *6*(24), e147170. https://doi.org/10.1172/jci.insight.147170

Martínez-Casales, M., Hernanz, R., & Alonso, M. J. (2021). Vascular and Macrophage Heme Oxygenase-1 in Hypertension: A Mini-Review. *Frontiers in Physiology*, *12*, 643435. https://doi.org/10.3389/fphys.2021.643435

MATUSZEWSKI, M., AFOLABI, A. A., ILESANMI, O. S., PRUC, M., NAVOLOKINA, A., AL-JEABORY, M., BORKOWSKA, M., NUCERA, G., YILDIRIM, M., CHIRICO, F., & SZARPAK, L. (2022). Associations between Interleukin-4 and COVID-19 severity: A systematic review and meta-analysis. *Journal of Health and Social Sciences*, *7*(4), 381. https://doi.org/10.19204/2022/SSCT4

Mazzocco, Y. L., Bergero, G., Del Rosso, S., Eberhardt, N., Sola, C., Saka, H. A., Villada, S. M., Bocco, J. L., & Aoki, M. P. (2023). Differential expression patterns of purinergic ectoenzymes and the antioxidative role of IL-6 in hospitalized COVID-19 patient recovery. *Frontiers in Immunology*, *14*, 1227873. https://doi.org/10.3389/fimmu.2023.1227873

McElvaney, O. J., Curley, G. F., Rose-John, S., & McElvaney, N. G. (2021). Interleukin-6: Obstacles to targeting a complex cytokine in critical illness. *The Lancet. Respiratory Medicine*, *9*(6), 643–654. https://doi.org/10.1016/S2213-2600(21)00103-X

Montazersaheb, S., Hosseiniyan Khatibi, S. M., Hejazi, M. S., Tarhriz, V., Farjami, A., Ghasemian Sorbeni, F., Farahzadi, R., & Ghasemnejad, T. (2022). COVID-19 infection: An overview on cytokine storm and related interventions. *Virology Journal*, *19*, 92. https://doi.org/10.1186/s12985-022-01814-1

O'Brien, S. A., Zhu, M., & Zhang, W. (2015). The Importance of IL-6 in the Development of LAT-Mediated Autoimmunity. *The Journal of Immunology*, *195*(2), 695–705. https://doi.org/10.4049/jimmunol.1403187

Oladunni, F. S., Park, J.-G., Pino, P. A., Gonzalez, O., Akhter, A., Allué-Guardia, A., Olmo-Fontánez, A., Gautam, S., Garcia-Vilanova, A., Ye, C., Chiem, K., Headley, C., Dwivedi, V., Parodi, L. M., Alfson, K. J., Staples, H. M., Schami, A., Garcia, J. I., Whigham, A., … Torrelles, J. B. (2020). Lethality of SARS-CoV-2 infection in K18 human angiotensin-converting enzyme 2 transgenic mice. *Nature Communications*, *11*(1), Article 1. https://doi.org/10.1038/s41467-020-19891-7

Orlov, M., Wander, P. L., Morrell, E. D., Mikacenic, C., & Wurfel, M. M. (2020). A Case for Targeting Th17 Cells and IL-17A in SARS-CoV-2 Infections. *Journal of Immunology (Baltimore, Md.: 1950)*, *205*(4), 892–898. https://doi.org/10.4049/jimmunol.2000554

Ouyang, W., & O'Garra, A. (2019). IL-10 Family Cytokines IL-10 and IL-22: From Basic Science to Clinical Translation. *Immunity*, *50*(4), 871–891. https://doi.org/10.1016/j.immuni.2019.03.020

Park, A., & Iwasaki, A. (2020). Type I and Type III Interferons – Induction, Signaling, Evasion, and Application to Combat COVID-19. *Cell Host & Microbe*, *27*(6), 870–878. https://doi.org/10.1016/j.chom.2020.05.008

Platanias, L. C. (2005). Mechanisms of type-I- and type-II-interferon-mediated signalling. *Nature Reviews Immunology*, *5*(5), Article 5. https://doi.org/10.1038/nri1604

Rabaan, A. A., Al-Ahmed, S. H., Muhammad, J., Khan, A., Sule, A. A., Tirupathi, R., Mutair, A. A., Alhumaid, S., Al-Omari, A., Dhawan, M., Tiwari, R., Sharun, K., Mohapatra, R. K., Mitra, S., Bilal, M., Alyami, S. A., Emran, T. B., Moni, M. A., & Dhama, K. (2021). Role of Inflammatory Cytokines in COVID-19 Patients: A Review on Molecular Mechanisms, Immune Functions, Immunopathology and Immunomodulatory Drugs to Counter Cytokine Storm. *Vaccines*, *9*(5), Article 5. https://doi.org/10.3390/vaccines9050436

Rashid, F., Xie, Z., Suleman, M., Shah, A., Khan, S., & Luo, S. (2022). Roles and functions of SARS-CoV-2 proteins in host immune evasion. *Frontiers in Immunology*, *13*. https://doi.org/10.3389/fimmu.2022.940756

Rubio-Casillas, A., Redwan, E. M., & Uversky, V. N. (2022). SARS-CoV-2: A Master of Immune Evasion. *Biomedicines*, *10*(6). https://doi.org/10.3390/biomedicines10061339

Sitia, R., & Rubartelli, A. (2018). The unconventional secretion of IL-1β: Handling a dangerous weapon to optimize inflammatory responses. *Seminars in Cell & Developmental Biology*, *83*, 12–21. https://doi.org/10.1016/j.semcdb.2018.03.011

Tjan, L. H., Furukawa, K., Nagano, T., Kiriu, T., Nishimura, M., Arii, J., Hino, Y., Iwata, S., Nishimura, Y., & Mori, Y. (2021). Early Differences in Cytokine Production by Severity of Coronavirus Disease 2019. *The Journal of Infectious Diseases*, *223*(7), 1145–1149. https://doi.org/10.1093/infdis/jiab005

Toro, A., Ruiz, M. S., Lage-Vickers, S., Sanchis, P., Sabater, A., Pascual, G., Seniuk, R., Cascardo, F., Ledesma-Bazan, S., Vilicich, F., Vazquez, E., & Gueron, G. (2022). A Journey into the Clinical Relevance of Heme Oxygenase 1 for Human Inflammatory Disease and Viral Clearance: Why Does It Matter on the COVID-19 Scene? *Antioxidants (Basel, Switzerland)*, *11*(2), 276. https://doi.org/10.3390/antiox11020276

Xu, S., Zhang, J., Liu, J., Ye, J., Xu, Y., Wang, Z., Yu, J., Ye, D., Zhao, M., Feng, Y., Pan, W., Wang, M., & Wan, J. (2021). The role of interleukin-10 family members in cardiovascular diseases. *International Immunopharmacology*, *94*, 107475. https://doi.org/10.1016/j.intimp.2021.107475

Yang, E., & Li, M. M. H. (2020). All About the RNA: Interferon-Stimulated Genes That Interfere With Viral RNA Processes. *Frontiers in Immunology*, *11*. https://www.frontiersin.org/articles/10.3389/fimmu.2020.605024

Yuen, C.-K., Wong, W.-M., Mak, L.-F., Lam, J.-Y., Cheung, L.-Y., Cheung, D. T.-Y., Ng, Y.-Y., Lee, A. C.-Y., Zhong, N., Yuen, K.-Y., & Kok, K.-H. (2023). An interferon-integrated mucosal vaccine provides pan-sarbecovirus protection in small animal models. *Nature Communications*, *14*, 6762. https://doi.org/10.1038/s41467-023-42349-5

Zhou, S., Lv, P., Li, M., Chen, Z., Xin, H., Reilly, S., & Zhang, X. (2023). SARS-CoV-2 E protein: Pathogenesis and potential therapeutic development. *Biomedicine & Pharmacotherapy*, *159*, 114242. https://doi.org/10.1016/j.biopha.2023.114242

Zizzo, G., Tamburello, A., Castelnovo, L., Laria, A., Mumoli, N., Faggioli, P. M., Stefani, I., & Mazzone, A. (2022). Immunotherapy of COVID-19: Inside and Beyond IL-6 Signalling. *Frontiers in Immunology*, *13*, 795315. https://doi.org/10.3389/fimmu.2022.795315